$$\dot{X}'(d) > \dot{X}(d) \qquad (2.48)$$

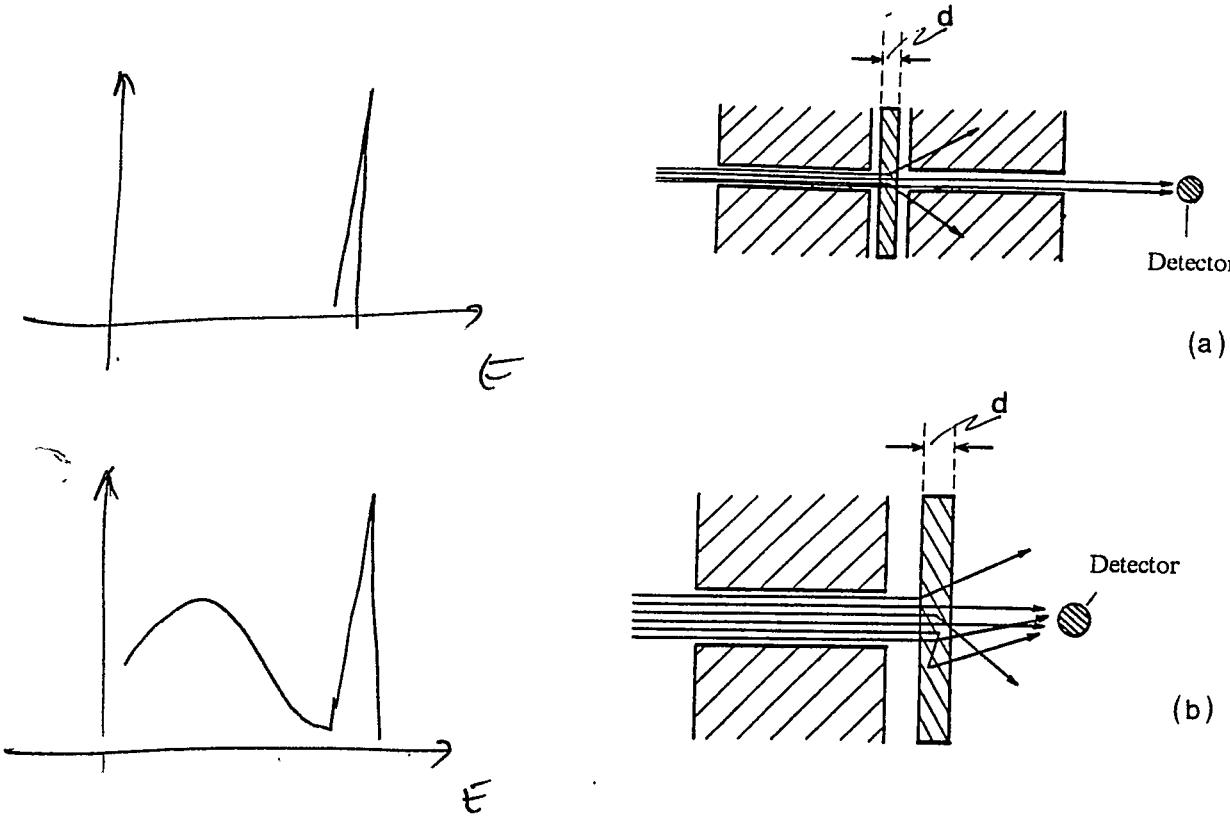

Fig. 2.8 Arrangement of shielding a beam of photons in (a) *good geometry* or *narrow beam*, and in (b) *bad geometry* or *broad beam*.

This situation is usually handled by defining the known as *buildup factors*.

For the case of the magnitude *exposure* or *exposure rate*, we have:

$$B_X(E_\gamma,\mu d) = \dot{X}'(d) / \dot{X}(d) \qquad (2.49)$$

the *exposure buildup factor*.

The values of the buildup factors, are depended on the magnitude to which are refered (flux, exposure, absorbed dose etc.), the shape of the photon beam (parallel or conical), the primary photons energy E_γ, the slab thickness (d) and the attenuation coefficient of the shielding material (μ).

In Table 2.6 are given values for the exposure buildup factor for the case of a parallel beam, as a function of energy for several materials and slab thicknesses.

Table 2.6 Exposure Buildup Factors for a Monodirectional Beam of Photons.

Material	E_0, MeV	$\mu_0 x$ 1	2	4	7	10	15
Water	0.5	2.63	4.29	9.05	20.0	35.9	74.9
	1.0	2.26	3.39	6.27	11.5	18.0	30.8
	2.0	1.84	2.63	4.28	6.96	9.87	14.4
	3.0	1.69	2.31	3.57	5.51	7.48	10.8
	4.0	1.58	2.10	3.12	4.63	6.19	8.54
	6.0	1.45	1.86	2.63	3.76	4.86	6.78
	8.0	1.36	1.69	2.30	3.16	4.00	5.47
Iron	0.5	2.07	2.94	4.87	8.31	12.4	20.6
	1.0	1.92	2.74	4.57	7.81	11.6	18.9
	2.0	1.69	2.35	3.76	6.11	8.78	13.7
	3.0	1.58	2.13	3.32	5.26	7.41	11.4
	4.0	1.48	1.90	2.95	4.61	6.46	9.92
	6.0	1.35	1.71	2.48	3.81	5.35	8.39
	8.0	1.27	1.55	2.17	3.27	4.58	7.33
	10.0	1.22	1.44	1.95	2.89	4.07	6.70
Tin	1.0	1.65	2.24	3.40	5.18	7.19	10.5
	2.0	1.58	2.13	3.27	5.12	7.13	11.0
	4.0	1.39	1.80	2.69	4.31	6.30	
	6.0	1.27	1.57	2.27	3.72	5.77	11.0
	10.0	1.16	1.33	1.77	2.81	4.53	9.68
Lead	0.5	1.24	1.39	1.63	1.87	2.08	
	1.0	1.38	1.68	2.18	2.80	3.40	4.20
	2.0	1.40	1.76	2.41	3.36	4.35	5.94
	3.0	1.36	1.71	2.42	3.55	4.82	7.18
	4.0	1.28	1.56	2.18	3.29	4.69	7.70
	6.0	1.19	1.40	1.87	2.97	4.69	9.53
	8.0	1.14	1.30	1.69	2.61	4.18	9.08
	10.0	1.11	1.24	1.54	2.27	3.54	7.70
Uranium	0.5	1.17	1.28	1.45	1.60	1.73	
	1.0	1.30	1.53	1.90	2.32	2.70	3.60
	2.0	1.33	1.62	2.15	2.87	3.56	4.89
	3.0	1.29	1.57	2.13	3.02	3.99	5.94
	4.0	1.25	1.49	2.02	2.94	4.06	6.47
	6.0	1.18	1.37	1.82	2.74	4.12	7.79
	8.0	1.13	1.27	1.61	2.39	3.65	7.36
	10.0	1.10	1.21	1.48	2.12	3.21	6.58

*From H. Goldstein, *Fundamental Aspects of Reactor Shielding*. Reading, Mass.: Addison-Wesley, 1959; now available from Johnson Reprint Corp., New York.

Thus, by using the buildup factors, the increased (buildup) magnitudes, for example $\dot{X}'$, is computed as follows:

$$\dot{X}' = \dot{X} \cdot B_X^{mb}(E_\gamma,\mu d) = 0.0659 \cdot E_\gamma \cdot (\mu_a/\rho)_{Air} \cdot I_0 \cdot e^{\mu d} \cdot B_X^{mb}(E_\gamma,\mu d) \qquad (2.50)$$

where: $B_X^{mb}(E_\gamma,\mu d)$, is the exposure (x) buildup factor for a monodirectional beam (^{mb}).

For the case of photons emerging from a point source [see Fig. 2.4 and equ. (2.28)], the increased (buildup) exposure rate at point P will be:

$$\dot{X}'(r,d) = \dot{X}(r,d) \cdot B_X^{ps}(E_\gamma,\mu d)$$

$$= 0.0659 \cdot E_\gamma \cdot (\mu_a/\rho)_{Air} \frac{S}{4\pi r^2} e^{\mu d} \cdot B_X^{ps}(E_\gamma,\mu d) \qquad (2.51)$$

where: $B_X^{ps}(E_\gamma,\mu d)$, is the exposure (x) buildup factor for the case of the isotropic point source (^{ps}).

Values for B_X^{ps} are given in Table 2.7.

2.8.1 Buildup flux.

By analogy to expressions (2.46) and (2.50), we may write for the exposure rate created by a point isotropical source:

$$\dot{X}(r,d) = 0.0659 \cdot E_\gamma \cdot (\mu_a/\rho)_{Air} \cdot \Phi(r,d) \quad \text{(mR/hr)} \qquad (2.52)$$

and:

$$\dot{X}'(r,d) = 0.0659 \cdot E_\gamma \cdot (\mu_a/\rho)_{Air} \cdot \Phi'(r,d) \quad \text{(mR/hr)} \qquad (2.53)$$

where: $\Phi(r,d)$ [see equ. (2.8)] is the flux of the uncollided photons of energy E_γ, from the source at distant r, after passing a shield of thickness d, and

$\Phi'(r,d)$ is a *"hypothetical flux"* of monoenergetic photons of energy E_γ, which gives the same exposure rate at the point P in Fig. 2.5, as the actual γ-ray flux at that point does. This quantity is called *"the buildup flux"*.

2.8.2 Mathematical models for the buildup factors.

For computational purposes it is convenient to express the buildup factor as a mathematical function. Several such functions have been developed. Some of them are given bellow.

a. The exponential form: $B(E_\gamma,\mu d) = A \cdot e^{\alpha_1 \mu d} + (1-A) \cdot e^{\alpha_2 \mu d}$ (2.54)

known as *the Taylor form.*

Table 2.7 Exposure Buildup Factors for an Isotropic Point Source.

Material	E_0, MeV	$\mu_0 r$ 1	2	4	7	10	15	20
Water	0.255	3.09	7.14	23.0	72.9	166	456	982
	0.5	2.52	5.14	14.3	38.8	77.6	178	334
	1.0	2.13	3.71	7.68	16.2	27.1	50.4	82.2
	2.0	1.83	2.77	4.88	8.46	12.4	19.5	27.7
	3.0	1.69	2.42	3.91	6.23	8.63	12.8	17.0
	4.0	1.58	2.17	3.34	5.13	6.94	9.97	12.9
	6.0	1.46	1.91	2.76	3.99	5.18	7.09	8.85
	8.0	1.38	1.74	2.40	3.34	4.25	5.66	6.95
	10.0	1.33	1.63	2.19	2.97	3.72	4.90	5.98
Aluminum	0.5	2.37	4.24	9.47	21.5	38.9	80.8	141
	1.0	2.02	3.31	6.57	13.1	21.2	37.9	58.5
	2.0	1.75	2.61	4.62	8.05	11.9	18.7	26.3
	3.0	1.64	2.32	3.78	6.14	8.65	13.0	17.7
	4.0	1.53	2.08	3.22	5.01	6.88	10.1	13.4
	6.0	1.42	1.85	2.70	4.06	5.49	7.97	10.4
	8.0	1.34	1.68	2.37	3.45	4.58	6.56	8.52
	10.0	1.28	1.55	2.12	3.01	3.96	5.63	7.32
Iron	0.5	1.98	3.09	5.98	11.7	19.2	35.4	55.6
	1.0	1.87	2.89	5.39	10.2	16.2	28.3	42.7
	2.0	1.76	2.43	4.13	7.25	10.9	17.6	25.1
	3.0	1.55	2.15	3.51	5.85	8.51	13.5	19.1
	4.0	1.45	1.94	3.03	4.91	7.11	11.2	16.0
	6.0	1.34	1.72	2.58	4.14	6.02	9.89	14.7
	8.0	1.27	1.56	2.23	3.49	5.07	8.50	13.0
	10.0	1.20	1.42	1.95	2.99	4.35	7.54	12.4
Tin	0.5	1.56	2.08	3.09	4.57	6.04	8.64	
	1.0	1.64	2.30	3.74	6.17	8.85	13.7	18.8
	2.0	1.57	2.17	3.53	5.87	8.53	13.6	19.3
	3.0	1.46	1.96	3.13	5.28	7.91	13.3	20.1
	4.0	1.38	1.81	2.82	4.82	7.41	13.2	21.2
	6.0	1.26	1.57	2.37	4.17	6.94	14.8	29.1
	8.0	1.19	1.42	2.05	3.57	6.19	15.1	34.0
	10.0	1.14	1.31	1.79	2.99	5.21	12.5	33.4
Lead	0.5	1.24	1.42	1.69	2.00	2.27	2.65	(2.73)
	1.0	1.37	1.69	2.26	3.02	3.74	4.81	5.86
	2.0	1.39	1.76	2.51	3.66	4.84	6.87	9.00
	3.0	1.34	1.68	2.43	3.75	5.30	8.44	12.3
	4.0	1.27	1.56	2.25	3.61	5.44	9.80	16.3
	5.1	1.21	1.46	2.08	3.44	5.55	11.7	23.6
	6.0	1.18	1.40	1.97	3.34	5.69	13.8	32.7
	8.0	1.14	1.30	1.74	2.89	5.07	14.1	44.6
	10.0	1.11	1.23	1.58	2.52	4.34	12.5	39.2
Uranium	0.5	1.17	1.30	1.48	1.67	1.85	2.08	
	1.0	1.31	1.56	1.98	2.50	2.97	3.67	
	2.0	1.33	1.64	2.23	3.09	3.95	5.36	(6.48)
	3.0	1.29	1.58	2.21	3.27	4.51	6.97	9.88
	4.0	1.24	1.50	2.09	3.21	4.66	8.01	12.7
	6.0	1.16	1.36	1.85	2.96	4.80	10.8	23.0
	8.0	1.12	1.27	1.66	2.61	4.36	11.2	28.0
	10.0	1.09	1.20	1.51	2.26	3.78	10.5	28.5

*From H. Goldstein, *Fundamental Aspects of Reactor Shielding.* Reading, Mass.: Addison-Wesley, 1959; now available from Johnson Reprint Corp., New York.

b. The linear form: $B(E_\gamma,\mu d) = 1 + k\cdot(\mu d)$ (2.55)

c. The quadratic form: $B(E_\gamma,\mu d) = 1 + \lambda\cdot(\mu d) + \lambda'\cdot(\mu d)^2$ (2.56)

d. The polynomial form: $B(E_\gamma,\mu d) = \sum_0^3 \beta_\nu\cdot(\mu d)^\nu$ (2.57)

e. The Berger form: $B(E_\gamma,\mu d) = 1 + C\cdot(\mu d)\cdot e^{D\cdot(\mu d)}$ (2.58)

In the above equations the coefficients A, α_1, α_2, k, λ, λ', β_ν, C and D are functions of the photon energy (E_γ), the shielding material, the type of the photon beam (monodirectional or conical), and of the magnitude on which are refered (exposure, or absorbed dose). The most popular from the above expressions, are the *Taylor* and the *Berger forms*, which are sufficiently accurate to be used in many practical, shielding problems.
Values for the coefficients A, α_1 and α_2 are given in Table 2.8, while in Table 2.9 are given values for k, λ, λ', C and D.

2.9 Shielding of gamma-ray sources.

The relations for the shielding of monodirectional beams of monoenergetic γ-rays, or γ-rays emitted from point isotropic sources, have already been given in paragraph 2.8. In the present paragraph we are going to describe mainly the case of shielding of distributed sources of various geometries.

2.9.1 Shielding of a point source by a slab of material.

We consider the point isotropic source of Fig. 2.9 emitting S γ-rays/sec, positioned behind a slab of material of thickness d. The uncollided flux at point P_1, lying on the line drawn from point S perpendicular to the slab, is

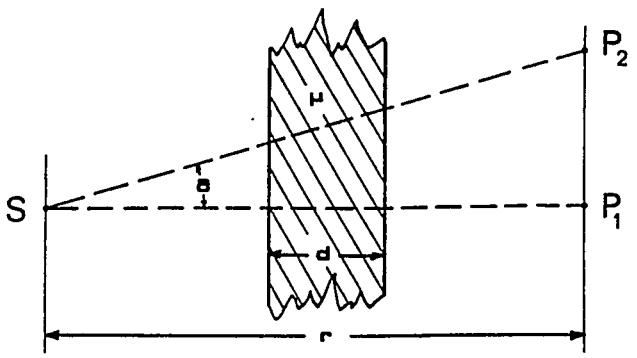

Fig. 2.9 Shielding of an isotropic point γ-ray source with a slab of material.

Table 2.8 Parameters for the Taylor form of the Exposure Buildup Factor for Point Isotropic Source.

Substance	Energy (MeV)	A	$-\alpha_1$	α_2	Substance	Energy (MeV)	A	$-\alpha_1$	α_2
Water	0.5	100.845	0.12687	−0.10925	**Iron**	0.5	31.379	0.06842	−0.03742
	1.0	19.601	0.09037	−0.02522		1.0	24.957	0.06086	−0.02463
	2.0	12.612	0.05320	0.01932		2.0	17.622	0.04627	−0.00526
	3.0	11.110	0.03550	0.03206		3.0	13.218	0.04431	−0.00087
	4.0	11.163	0.02543	0.03025		4.0	9.624	0.04698	0.00175
	6.0	8.385	0.01820	0.04164		6.0	5.867	0.06150	−0.00186
	8.0	4.635	0.02633	0.07097		8.0	3.243	0.07500	0.02123
	10.0	3.545	0.02991	0.08717		10.0	1.747	0.09900	0.06627
Concrete	0.5	38.225	0.14824	−0.10579	**Tin**	0.5	11.440	0.01800	0.03187
	1.0	25.507	0.07230	−0.01843		1.0	11.426	0.04266	0.01606
	2.0	18.089	0.04250	0.00849		2.0	8.783	0.05349	0.01505
	3.0	13.640	0.03200	0.02022		3.0	5.400	0.07440	0.02080
	4.0	11.460	0.02600	0.02450		4.0	3.496	0.09517	0.02598
	6.0	10.781	0.01520	0.02925		6.0	2.005	0.13733	−0.01501
	8.0	8.972	0.01300	0.02979		8.0	1.101	0.17288	−0.01787
	10.0	4.015	0.02880	0.06844		10.0	0.708	0.19200	0.01552
Aluminum	0.5	38.911	0.10015	−0.06312	**Lead**	0.5	1.677	0.03084	0.30941
	1.0	28.782	0.06820	−0.02973		1.0	2.984	0.03503	0.13486
	2.0	16.981	0.04588	0.00271		2.0	5.421	0.03482	0.04379
	3.0	10.583	0.04066	0.02514		3.0	5.580	0.05422	0.00611
	4.0	7.526	0.03973	0.03860		4.0	3.897	0.08468	−0.02383
	6.0	5.713	0.03934	0.04347		6.0	0.926	0.17860	−0.04635
	8.0	4.716	0.03837	0.04431		8.0	0.368	0.23691	−0.05864
	10.0	3.999	0.03900	0.04130		10.0	0.311	0.24024	−0.02783

*From H. Goldstein, *Fundamental Aspects of Reactor Shielding.* Reading, Mass.: Addison-Wesley, 1959; now available from Johnson Reprint Corp., New York.

Table 2.9a Coefficients for Linear, Quadratic and Berger forms of Exposure Buildup Factors, fitted over the range 0 to 7 mean free paths from Point Isotropic Source.

		Linear		Quadratic			Berger		
Material	E, MeV	A_1	Maximum error,‡ %	A_2	b	Maximum error, %	C	D	Maximum error, %
Water	0.255	8.6524	F3.1	−0.2525	1.4984	30	1.7506	0.2609	10
	0.5	4.6800	F2.3	0.6684	0.6750	8	1.3245	0.2078	5
	1	1.9953	40	1.0053	0.1666	2	1.0622	0.1052	3
	2	1.0301	10	0.8242	0.0346	2	0.8093	0.0408	1
	3	0.7397	3	0.6962	0.0073	1	0.6876	0.0125	1
	4	0.5884	1	0.5801	0.0014	1	0.5800	0.0024	1
	6	0.4321	3	0.4616	−0.0050	1	0.4655	−0.0126	1
	8	0.3406	4	0.3782	−0.0063	1	0.3860	−0.0214	1
	10	0.2877	4	0.3251	−0.0063	1	0.3342	−0.0257	1
Aluminum	0.5	2.6461	F1.5	1.0688	0.2654	2	1.2435	0.1250	3
	1	1.6089	30	0.9316	0.1140	2	0.9589	0.0864	3
	2	0.9686	13	0.7437	0.0378	2	0.7267	0.0486	2
	3	0.7197	5	0.6355	0.0142	1	0.6294	0.0227	1
	4	0.5663	3	0.5284	0.0064	1	0.5253	0.0127	1
	6	0.4334	2	0.4142	0.0032	1	0.4177	0.0061	1
	8	0.3476	1	0.3346	0.0022	1	0.3371	0.0050	1
	10	0.2847	2	0.2715	0.0022	1	0.2752	0.0055	1
Iron	0.5	1.4283	25	0.8642	0.0949	1	0.9081	0.0752	2
	1	1.2373	20	0.8026	0.0731	1	0.8214	0.0684	2
	2	0.8556	12	0.6526	0.0342	5	0.7020	0.0319	3
	3	0.6691	9	0.5338	0.0228	1	0.5323	0.0384	1
	4	0.5403	7	0.4366	0.0175	1	0.4366	0.0358	1
	6	0.4297	8	0.3237	0.0178	1	0.3271	0.0457	1
	8	0.3391	8	0.2473	0.0154	1	0.2563	0.0464	1
	10	0.2681	8	0.1785	0.0151	1	0.1876	0.0592	1
Tin	0.5	0.5153	3	0.5479	−0.0055	2	0.5608	−0.0146	1
	1	0.7199	6	0.6153	0.0176	1	0.6219	0.0244	1
	2	0.6731	8	0.5455	0.0215	1	0.5498	0.0338	1
	3	0.5837	11	0.4284	0.0261	1	0.4379	0.0479	1
	4	0.5146	12	0.3420	0.0290	1	0.3583	0.0601	1
	6	0.4153	17	0.2082	0.0348	2	0.2369	0.0925	1
	8	0.3317	17	0.1371	0.0327	2	0.1692	0.1103	1
	10	0.2550	16	0.0945	0.0270	2	0.1232	0.1190	1
Tungsten	0.5	0.1903	8	0.2692	−0.0133	2	0.2938	−0.0751	2
	1	0.3817	5	0.4269	−0.0076	2	0.4425	−0.0255	1
	2	0.4376	2	0.4164	0.0036	1	0.4172	0.0080	1
	3	0.4171	5	0.3515	0.0110	1	0.3501	0.0295	1
	4	0.4054	12	0.2540	0.0255	1	0.2710	0.0666	1
	6	0.3363	17	0.1435	0.0324	2	0.1771	0.1049	1
	8	0.2624	16	0.0957	0.0281	2	0.1245	0.1223	1
	10	0.2073	14	0.0748	0.0223	2	0.0974	0.1238	1
Lead	0.5	0.1549	8	0.2273	−0.0122	3	0.2526	−0.0848	2
	1	0.2990	6	0.3613	−0.0105	2	0.3779	−0.0403	1
	2	0.3796	1	0.3787	0.0001	1	0.3862	0.0032	1
	3	0.3810	5	0.3164	0.0109	1	0.3267	0.0253	1
	4	0.3523	10	0.2389	0.0191	1	0.2530	0.0547	1
	5.1	0.3219	13	0.1747	0.0248	1	0.1936	0.0839	1
	6	0.3034	15	0.1346	0.0284	2	0.1622	0.1027	1
	8	0.2419	15	0.0894	0.0257	3	0.1220	0.1112	2
	10	0.1933	13	0.0642	0.0217	3	0.0939	0.1167	2
Uranium	0.5	0.1054	7	0.1637	−0.0098	2	0.1825	−0.0951	2
	1	0.2264	7	0.2990	−0.0122	2	0.3204	−0.0599	2
	2	0.3023	3	0.3250	−0.0038	1	0.3321	−0.0162	1
	3	0.3169	4	0.2760	0.0069	1	0.2814	0.0196	1
	4	0.3010	7	0.2199	0.0136	1	0.2283	0.0458	1
	6	0.2571	12	0.1314	0.0212	1	0.1476	0.0916	1
	8	0.2081	12	0.0885	0.0201	1	0.1081	0.1076	1
	10	0.1621	11	0.0638	0.0165	1	0.0798	0.1163	1

†From D. K. Trubey, A Survey of Empirical Functions Used To Fit Gamma-Ray Buildup Factors, USAEC Report ORNL-RSIC-10, Oak Ridge National Laboratory, February 1966.

‡F3.1 means "factor of 3.1," etc.

Table 2.9b Coefficients for Linear, Quadratic and Berger forms of Exposure Buildup Factors, fitted over the range 0 to 20 mean free paths from Point Isotropic Sources.

		Linear		Quadratic			Berger		
Material	E, MeV	A_1	Maximum error,‡ %	A_2	b	Maximum error, %‡	C	D	Maximum error, %
Water	0.255	36.1015	F12	−12.9947	3.0515	F∞	2.5048	0.1623	30
	0.5	13.0926	F5.6	−0.9744	0.8743	F3	1.8035	0.1224	25
	1	3.4788	F2	1.1152	0.1469	6	1.2282	0.0649	11
	2	1.2549	25	0.9173	0.0210	6	0.8594	0.0240	5
	3	0.7863	6	0.7218	0.0040	2	0.7004	0.0074	2
	4	0.5951	1	0.5907	0.0003	1	0.5826	0.0014	1
	6	0.4030	5	0.4471	−0.0027	2	0.4853	−0.0082	1
	8	0.3085	7	0.3561	−0.0038	2	0.3741	−0.0124	2
	10	0.2584	7	0.3002	−0.0026	3	0.3206	−0.0139	2
Aluminum	0.5	5.7374	F3	0.6696	0.3150	20	1.4412	0.0850	12
	1	2.5385	F1.9	1.1185	0.0883	10	1.0831	0.0535	9
	2	1.1928	30	0.8751	0.0197	8	0.7869	0.0266	6
	3	0.8061	12	0.6812	0.0078	3	0.6504	0.0137	3
	4	0.6075	6	0.5503	0.0036	2	0.5343	0.0082	2
	6	0.4626	6	0.4252	0.0023	2	0.4182	0.0063	1
	8	0.3697	5	0.3395	0.0019	1	0.3366	0.0058	1
	10	0.3087	5	0.2750	0.0021	1	0.2738	0.0074	1
Iron	0.5	2.3773	F1.9	0.9019	0.0917	3	0.9814	0.0548	7
	1	1.8643	F1.6	0.9212	0.0586	7	0.8932	0.0460	7
	2	1.1194	33	0.7423	0.0234	6	0.7173	0.0277	4
	3	0.8446	25	0.5840	0.0162	4	0.5571	0.0261	4
	4	0.6942	25	0.4605	0.0145	2	0.4518	0.0268	3
	6	0.6134	34	0.3201	0.0182	1	0.3381	0.0368	3
	8	0.5245	40	0.2207	0.0189	3	0.2603	0.0428	2
	10	0.4759	50	0.1143	0.0225	6	0.1902	0.0553	1
Tin	0.5	0.5090	4	0.5150	−0.0005	3	0.5457	−0.0063	3
	1	0.8495	18	0.6666	0.0114	3	0.6378	0.0180	3
	2	0.8521	25	0.5826	0.0168	3	0.5678	0.0254	3
	3	0.8509	40	0.4254	0.0264	1	0.4533	0.0388	3
	4	0.8643	F1.58	0.2845	0.0360	5	0.3700	0.0518	3
	6	1.0786	F2.2	−0.1374	0.0756	40	0.2401	0.0891	2
	8	1.1907	F2.8	−0.4693	0.1032	F3	0.1669	0.1145	1
	10	1.1075	F3.0	−0.6523	0.1094	F12	0.1190	0.1278	5
Tungsten	0.5	0.1550	13	0.2206	−0.0054	5	0.2692	−0.0477	5
	1	0.3382	9	0.4149	−0.0048	2	0.4279	−0.0150	2
	2	0.4671	8	0.4072	0.0037	3	0.4163	0.0070	4
	3	0.5919	30	0.3255	0.0165	2	0.3484	0.0324	2
	4	0.8102	F1.8	0.0995	0.0442	15	0.2727	0.0653	1
	6	1.2616	F3	−0.5462	0.1124	F4	0.1704	0.1160	2
	8	1.3753	F3.5	−0.9399	0.1439	F∞	0.1161	0.1405	6
	10	1.2730	F3.8	−0.9502	0.1382	F∞	0.0882	0.1510	7
Lead	0.5	0.1043	15	0.1791	−0.0047	5	0.2243	−0.0500	5
	1	0.2549	11	0.3133	−0.0036	5	0.3530	−0.0211	4
	2	0.3947	3	0.3695	0.0015	2	0.3791	0.0021	1
	3	0.5123	30	0.2990	0.0133	2	0.3244	0.0279	1
	4	0.6378	F1.6	0.1449	0.0306	10	0.2526	0.0557	1
	5.1	0.8560	F2.1	−0.1480	0.0624	40	0.1904	0.0883	2
	6	1.1247	F2.8	−0.5070	0.1014	F4	0.1554	0.1143	4
	8	1.4165	F4	−1.1408	0.1589	F∞	0.1075	0.1440	12
	10	1.2370	F4	−1.0279	0.1408	F∞	0.0824	0.1513	12
Uranium	0.5	0.0812	11	0.1262	−0.0037	5	0.1635	−0.0606	5
	1	0.1914	11	0.2556	−0.0053	5	0.2991	−0.0385	5
	2	0.2838	5	0.3185	−0.0022	2	0.3240	−0.0084	2
	3	0.4081	20	0.2614	0.0091	2	0.2781	0.0234	1
	4	0.4991	43	0.1621	0.0210	6	0.2273	0.0475	1
	6	0.8088	F2.3	−0.2492	0.0658	F2	0.1426	0.1011	2
	8	0.9323	F2.9	−0.5357	0.0912	F5	0.1004	0.1274	5
	10	0.9203	F3.3	−0.6560	0.0980	F∞	0.0721	0.1442	7

†From D. K. Trubey, A Survey of Empirical Functions Used To Fit Gamma-Ray Buildup Factors, USAEC Report ORNL-RSIC-10, Oak Ridge National Laboratory, February 1966.

‡F12 means "factor of 12," etc.

given by equ. (2.28),

$$\Phi_1(r,d) = \frac{S}{4\pi r^2} e^{-\mu d} \tag{2.59}$$

The same magnitude at another point P_2 is given by,

$$\Phi_2(r\sec\theta, d\sec\theta) = \frac{S}{4\pi (r\cdot\sec\theta)^2} e^{-\mu d\sec\theta} \tag{2.60}$$

while the buildup flux and the buildup rate of exposure, are given correspondingly by:

$$\Phi_2'(r\cdot\sec\theta, d\cdot\sec\theta) = S\cdot G_\Phi(r\cdot\sec\theta, d\cdot\sec\theta) \tag{2.61}$$

$$\dot{X}_2'(r\cdot\sec\theta, d\cdot\sec\theta) = S\cdot G_X(r\cdot\sec\theta, d\cdot\sec\theta) \tag{2.62}$$

where the functions,

$$G_\Phi(r\sec\theta, d\sec\theta) = B_X^{ps}(E_\gamma, \mu d\sec\theta)\cdot\frac{e^{-\mu d\sec\vartheta}}{4\pi (r\cdot\sec\vartheta)^2} \tag{2.63}$$

and,

$$G_X(r\sec\theta, d\sec\theta) = B_X^{ps}(E_\gamma, \mu d\sec\theta)\, 0.0659\, E_\gamma\cdot\left(\frac{\mu_a}{\rho}\right)_{Air}\cdot\frac{e^{-\mu d\sec\vartheta}}{4\pi (r\cdot\sec\vartheta)^2}$$

$$= 0.0659\, E_\gamma\left(\frac{\mu_a}{\rho}\right)_{Air} G_\Phi(r\sec\theta, d\sec\theta) \tag{2.64}$$

are known as *the point kernels* for *the flux* and *the exposure rate* correspondingly.

The physical meaning of the point kernels is, that they express the corresponding buildup magnitudes (flux and expossure rate) for a *unit intensity source* ($S_0 = 1$ photon/sec).
The point kernels, known also as *Green functions*, provide the means for solving a variety of problems that involve distributed sources.

2.9.2 Shielding of a line isotropic source, by an infinite slab.

We consider the case of a line source, of length L (cm) and of intensity S_L (γ-rays/cm sec), shielded by an infinite slab of thickness d, parallel to the line source, as is shown in Fig. 2.10. Considering the elementary source of intensity $S_L\, dL$ (γ-rays/sec) corresponding to the differential length dL of the source, as a point isotropic source, we may express the elementary buildup flux, or exposure rate at point P, as below:

$$d\Phi_1' = (S_L\cdot dL)\cdot G_\Phi(r\cdot\sec\theta, d\cdot\sec\theta) \tag{2.65}$$

$$d\dot{X}_1' = (S_L\cdot dL)\cdot G_X(r\cdot\sec\theta, d\cdot\sec\theta) \tag{2.66}$$

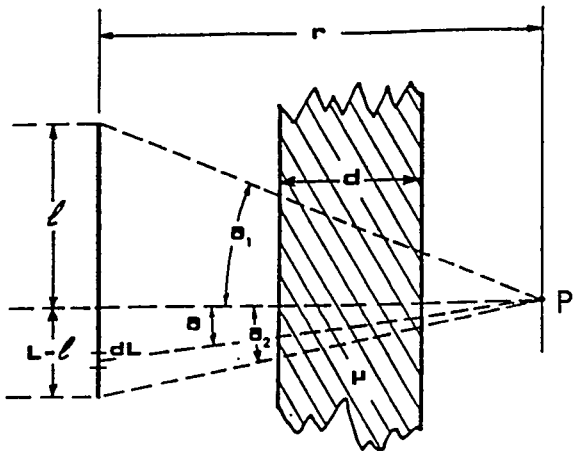

Fig. 2.10 Shielding of a line isotropic γ-ray source, with a slab of material.

where: $$dL = r \cdot \sec^2\theta \cdot d\theta \qquad (2.67)$$

By integrating equations (2.65) and (2.66) between the angles $\theta_1 = \arctan(1/r)$ and $\theta_2 = \arctan[(L - l)/r]$ we obtain for the buildup flux and the buildup exposure rate at point P, caused by the whole line source:

$$\Phi'_P = \frac{S_L}{4\pi r} \cdot \int_{\vartheta_1}^{\vartheta_2} B_x^{ps}(E_\gamma, \mu d \sec\vartheta) \cdot e^{-\mu d \sec\vartheta} \cdot d\vartheta \qquad (2.68)$$

$$\dot{X}'_P = 0.0659 \cdot E_\gamma \cdot \left(\frac{\mu_a}{\rho}\right)_{Air} \cdot \Phi'_P \qquad \text{(mR/hr)} \qquad (2.69)$$

In order to complete the integration, it is necessary to use an expression for the buildup factor. By using for example, the *Taylor form* [equ. (2.54)], we obtain for the buildup flux:

$$\Phi'_P = \frac{S_L}{4\pi r} \cdot \{A \cdot [F(\theta_1,\mu_1 d) + F(\theta_2,\mu_1 d)] + (1-A) \cdot [F(\theta_1,\mu_2 d) + F(\theta_2,\mu_2 d)]\} \qquad (2.70)$$

where: $$\mu_1 = (1+\alpha_1) \cdot \mu \qquad (2.71)$$
$$\mu_2 = (1+\alpha_2) \cdot \mu \qquad (2.72)$$

and, $$F(\theta, \mu d) = \int_0^{\vartheta} e^{-\mu d \sec\vartheta'} \cdot d\vartheta' \qquad (2.73)$$

the known as *Sievert integral function.*

Graphs of the Sievert function are found in the literature. One example is given in Fig. 2.11.

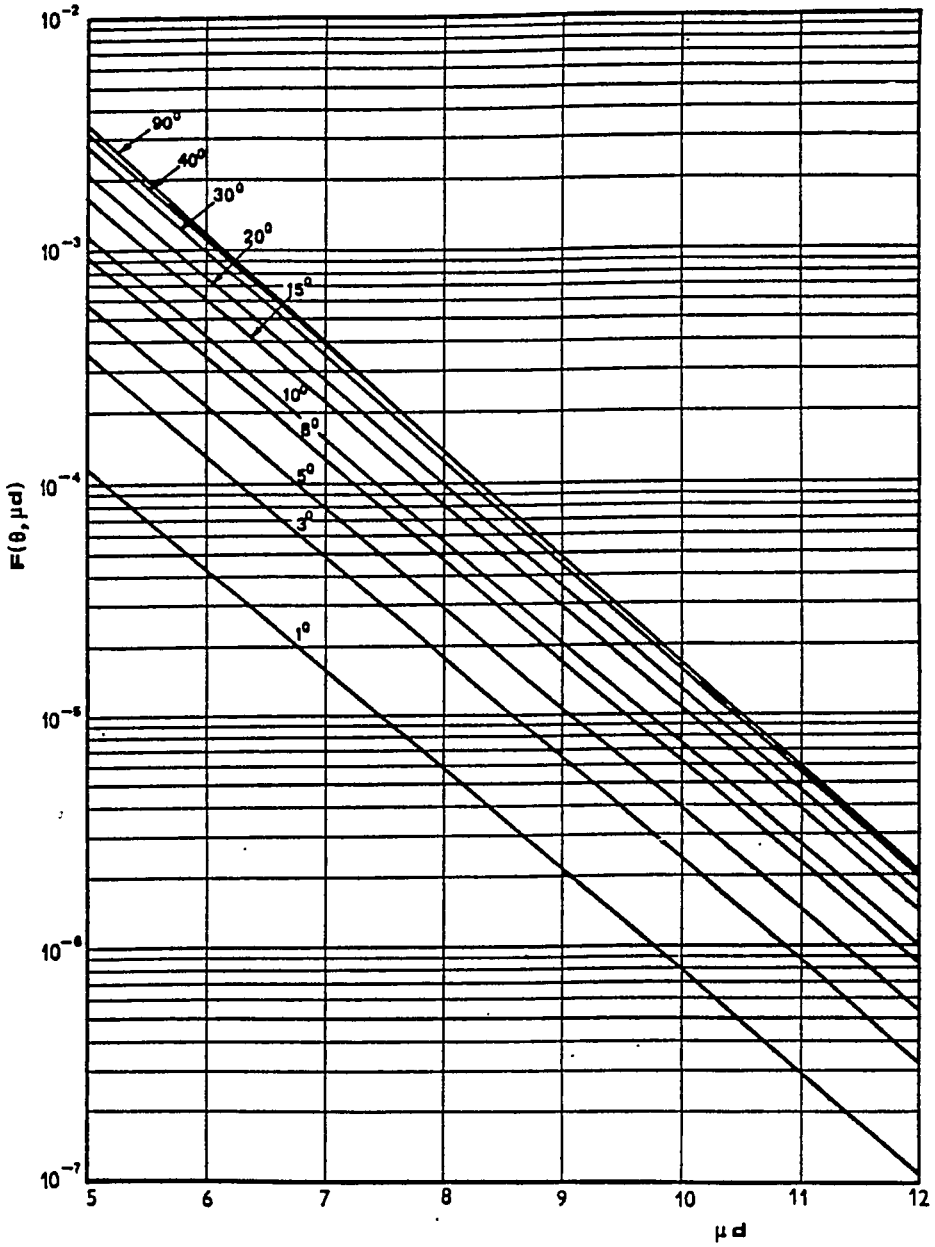

Fig. 2.11 Graphs of the Sievert integral function $F(\theta,\mu d)$ for $\theta = 1^o \div 90^o$ and $\mu d = 5 \div 12$.

For $\theta_1 = \theta_2 = \theta$, equation (2.70) gives:

$$\Phi_P' = \frac{S_L}{2\pi r}\cdot[A\cdot F(\theta, \mu_1 d) + (1 - A)\cdot F(\theta, \mu_2 d)] \qquad (2.74)$$

For an infinite line source, i.e. when $\theta_1 = \theta_2 = \pi/2$, equ. (2.70) gives:

$$\Phi_P = \frac{S_L}{2\pi r}\cdot[A\cdot F(\pi/2, \mu_1 d) + (1 - A)\cdot F(\pi/2, \mu_2 d)] \qquad (2.75)$$

2.9.3 Shielding of an isotropic disc source, with an infinite slab.

We consider the planar isotropic disk source of gamma-rays, of radius R and intensity S_S (γ-rays/cm^2 sec), shielded with an infinite slab of thickness d, parallel to the plane of the source, as is shown in Fig. 2.12.

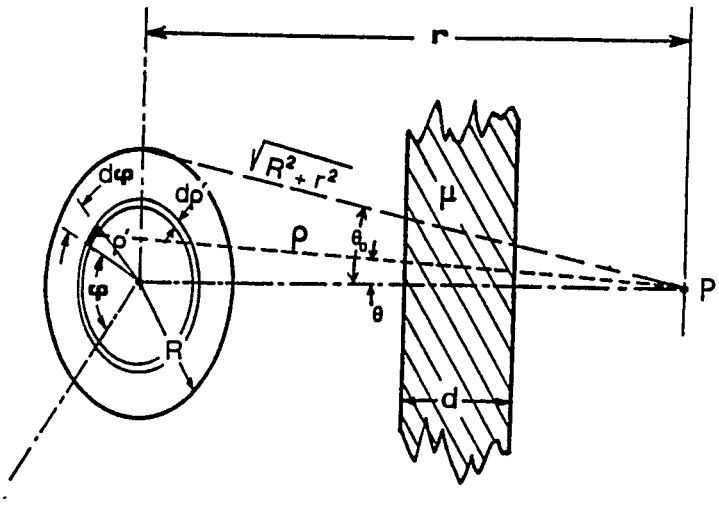

Fig. 2.12 Shielding of an isotropic planar disc source, by a slab of material.

We will compute the buildup flux at point P located along the axis of the disc. Consider the elementary source dS_S located in the annular region between ρ' and $\rho' + d\rho'$ and between the angles φ and $\varphi + d\varphi$. Its intensity is $S_S \cdot dS_S$ (γ-rays/sec), where:

$$dS_S = \rho' d\varphi \cdot d\rho' = \rho \cdot d\rho \cdot d\varphi \quad (cm^2) \tag{2.76}$$

The elementary buildup flux at point P is:

$$d\Phi'_P = S_S \cdot dS_S \cdot G_\Phi \tag{2.77}$$

where G_Φ is the *point kernel for the flux* and is given by equ. (2.63). Equ. (2.77) is thus written as:

$$d\Phi_P = S_S \cdot \rho \cdot d\rho \cdot d\varphi \cdot B_X^{ps}(E_\gamma, \mu d \sec\theta) \cdot \frac{e^{-\mu d \sec\vartheta}}{4\pi (r \cdot \sec\vartheta)^2} \tag{2.78}$$

By using the *Taylor form* for the buildup factor and integrating equ. (2.78) between the limits $0 \div 2\pi$ for φ and between $r \div \sqrt{r^2 + R^2}$ for $\rho = r \cdot \sec\theta$ we find:

$$\Phi'_P = \frac{S_s}{2}\{ A\cdot[E_1(\mu_1 d) - E_1(\mu_1 d\sec\theta_0) + (1-A)\cdot[E_1(\mu_2 d) - E_1(\mu_2 d\sec\theta_0)]\} \quad (2.79)$$

where: $\mu_1 = (1 + \alpha_1)\cdot\mu$ (2.80)

$\mu_2 = (1 + \alpha_2)\cdot\mu$ (2.81)

and $E_1(x) = \int_x^\infty \frac{e^{-t}}{t}.dt$ (2.82)

the known as *exponential integral function** of the first order.

Graphs of $E_1(x)$ are given in the literature. One example is given in Fig. 2.13.

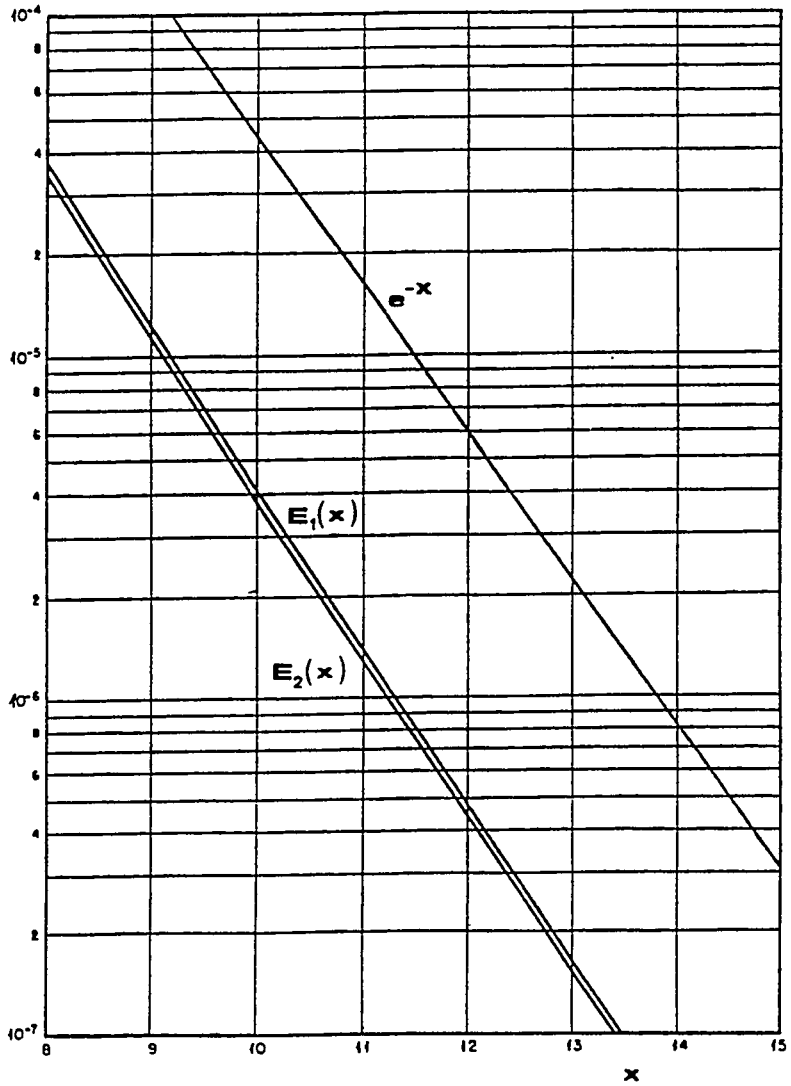

Fig. 2.13 Graphs of functions e^{-x}, $E_1(x)$ and $E_2(x)$ for $x = 8 \div 15$.

* In general the exponential integral function of n-th order, has as follows:

$$E_n = x^{n-1}\cdot\int_x^\infty e^{-y}.y^{-n}.dy$$

For $\theta_0 = \pi/2$, i.e. for the case of an infinite planar source, equ. (2.78) gives:

$$\Phi'_{P,\infty} = \frac{S_s}{2} \cdot [A \cdot E_1(\mu_1 d) + (1 - A) \cdot E_1(\mu_2 d)] \qquad (2.83)$$

2.9.4 Multilayered shields.

We consider in this paragraph the case of shields composed of more than one slab of material, as in Fig. 2.14.

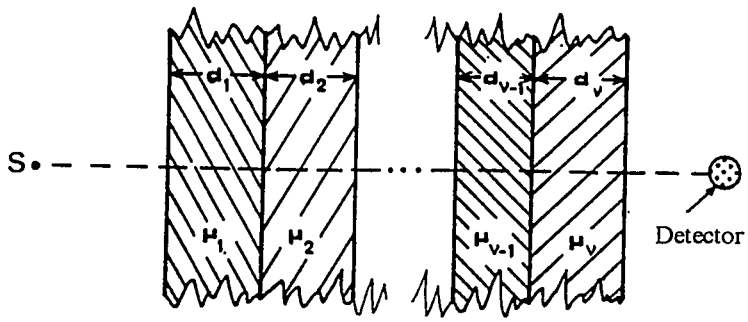

Fig. 2.14 Shielding of an isotopic point source by slabs of various materials.

The probability *a photon from the source to pass uncollided the slabs and reach the detector*, is given by the product of the partial probabilities, i.e.:

$$p(d_1, d_2, \ldots, d_v) = e^{-\mu_1 d_1} e^{-\mu_2 d_2} \ldots e^{-\mu_v d_v} = e^{-\sum_i^v \mu_i d_i} \qquad (2.84)$$

The theoretical calculation of the buildup magnitude of interest, the flux for example, at the point where the detector is positioned, presents problems mainly because of the difficulty in the expression of the buildup factor. The problem stems from the fact that buildup factors have been computed only for monoenergetic photons, incident on various materials. While these buildup factors can be used to describe the radiation leaving the first slab, they are not appropriate for the radiation leaving the second slab, and this, because the radiation incident on this slab, has a continuous spectrum resulting from interactions in the first layer, and so on.
Approximate values for the *multilayered shield buildup factor* can be obtained by using the following "recipies" which are based on qualitative arguments and extensive experimentation.

a. If after a slab of light material (water for example), follows a slab of heavy material (iron or lead for example), then it is recommended to use the buildup factor of the second medium, as if the first medium were not present. That means that we may use for the multilayered shield only $B_2(E_\gamma, \mu_2 d_2)$. This is justified from the fact that the low energy buildup

radiation from region-1, is absorbed in region-2.

b. In the case where the heavy material precedes the light material, the procedure to be followed depends upon whether the γ-ray energy (E_γ) is above or below the minimum in the μ-curve, which occurs at about 3 MeV for heavy elements (see Fig. 2.4). If $E_\gamma < 3$ MeV, it is recommended to calculate:

$$B_{1.2} = B_1(E_\gamma, \mu_1 d_1) \cdot B_2(E_\gamma, \mu_2 d_2) \tag{2.85}$$

This is justified by the fact that the energy of the photons emerging from a high-Z shield is little different from that of the source, and in the second medium the photons can be treated as if they were *source γ-rays.*

On the other hand, if $E_\gamma > 3$ MeV, then it is recommended to calculate:

$$B_{1.2} = B_1(E_\gamma, \mu_1 d_1) \cdot B_2(E_{min}, \mu_2 d_2) \tag{2.86}$$

where, $B_2(E_{min}, \mu_2 d_2)$ is the value of the buildup factor for the second (light material) slab, *taken at energie E_{min}, which corresponds to the minimum of μ in the curve $\mu(E_\gamma)$.* For lead for example, $E_{min} \simeq 3.2$ MeV. The recommendation of equ. (2.86) is based on the fact that the γ-rays penetrating the first slab, have energies clustered about the minimum in μ, so that their penetration through the second slab is determined by this energy rather, than by the actual source photons energy.

c. For the case of two or more than two slabs, *where the last one has thickness larger than two mean ranges* [see equ. (2.22)], i.e. $d_v > 2/\mu_v$, or $\mu_v \cdot d_v > 2$, *Blizard* recommends to use as buildup factor, the one corresponding to *the last slab material for the parameter $\mu \cdot d$*:

$$\mu \cdot d = \sum_{i}^{v} \mu_i \cdot d_i \tag{2.87}$$

This procedure is known as *Blizard's method*.

It is emphasized that the above mentioned recommendations, give only approximate results for the attenuation of gamma-rays in multilayered shields, and they are applied in the absence of exact methods of calculation, like the *Monte Carlo method* for example.

2.9.5 Slab source shielded by a slab of material.

We consider the case of Fig. 2.15, where a slab source of gamma-rays, of thickness h is shielded by a slab of material, placed parallel to the slab source. The source has generally, intensity $S_v(x)$ γ-rays of energy E_γ / cm^3.sec, where:

$$S_v(x) = S_v \text{ (constant)} , \tag{2.88}$$

or, $$S_V(x) = S_{V,0} \cdot e^{\alpha x}, \quad (\alpha > 0 \text{ or } \alpha < 0) \tag{2.89}$$

or, $$S_V(x) = S_{V,0} \cdot (1 + mx), \quad (m > 0 \text{ or } m < 0) \tag{2.90}$$

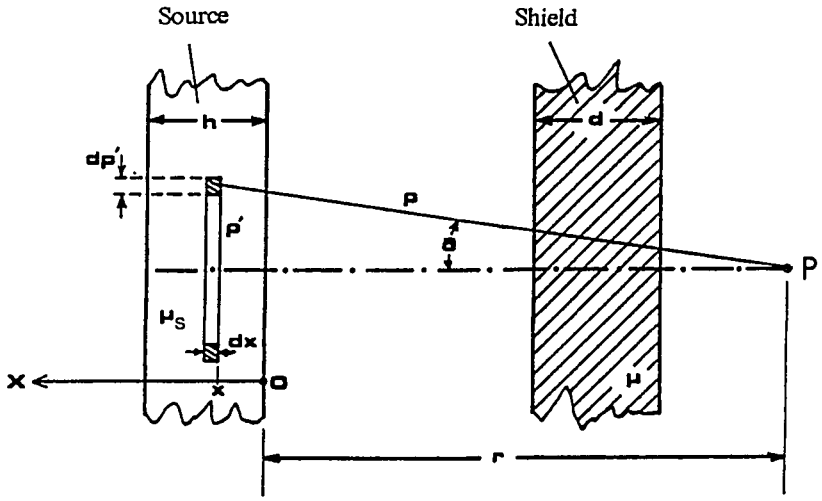

Fig. 2.15 Slab γ-ray source shielded with a parallel slab of material.

For the calculation of the buildup flux at point P, we follow the usual procedure. We express the elementary buildup flux at P, due to the elementary source of volume $dV = 2\pi \cdot \rho' \cdot d\rho' \cdot dx$, as:

$$d\Phi'_P = [S_V(x) \cdot dV] \cdot G_{\Phi,m} \tag{2.91}$$

where $G_{\Phi,m}$, is *the point kernel function, taking in account the attenuation in the source material also*. Thus, instead of equ. (2.63), and in the case that *Blizard's* presupposition holds (i.e. $\mu d > 2$), we should use the following point kernel expression:

$$G_{\Phi,m} = B_X^{PS}[(\mu d + \mu_s x)\sec\theta] \cdot \frac{e^{-(\mu d + \mu_s x)\cdot \sec\theta}}{4\pi (r+x)^2 \cdot \sec^2\theta} \tag{2.92}$$

where μ_s is *the linear attenuation coefficient of the source material.*

By using for the buildup factor, the *Taylor form*, we get for example for the case of $S_V(x) = S_V$ = constant,

$$\Phi'_P = \frac{S_V}{2\mu_S} \cdot \left\{ \frac{A}{1+a_1} \cdot \left[E_2[(1+a_1)\mu d] - E_2[(1+a_1)\cdot(\mu d + \mu_s h)] \right] \right.$$

$$\left. + \frac{1-A}{1+a_2} \cdot \left[E_2[(1+a_2)\mu d - E_2[(1+a_2)\cdot(\mu d + \mu_s h)] \right] \right\} \tag{2.93}$$

For $h \to \infty$ (i.e. for the semi-infinite source medium), we get:

$$\Phi'_{P,\infty} = \frac{S_V}{2\mu_S} \cdot \left\{ \frac{A}{1+a_1} \cdot E_2[(1+a_1)\mu d] + \right.$$

$$\left. + \frac{1-A}{1+a_2} \cdot E_2[(1+a_2)\mu a] \right\} \qquad (2.94)$$

2.9.6 Cylindrical source, shielded by a slab parallel to its axis.

We consider the homogeneous cylindrical source of hight L, radius R and of intensity S_V monoenergetic γ-rays per cm^3 per sec, shielded with a slab of material of thickness d, as is shown in Fig. 2.16.

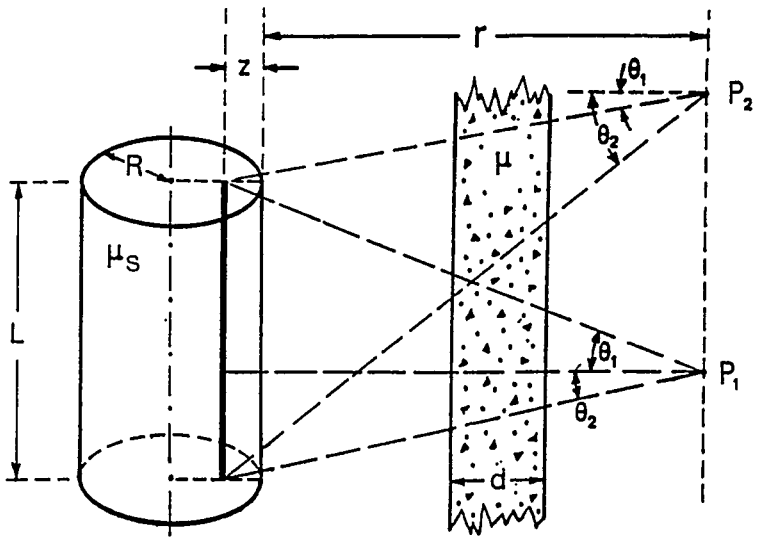

Fig. 2.16 Cylindrical gamma ray source, shielded with a slab of material, positioned parallel to its axis.

For the calculation of the buildup flux at some point P_1 or P_2, it is recommended to follow the approximation method described below.

In this approximation, the cylindrical source is replaced by an *equivalent isotropic linear source whose hight equals that of the cylinder.* The intensity of this source is $S_L = \pi \cdot R^2 \cdot S_V$, while its position is determined by the *self-absorption distance z* (see Fig. 2.16). This distance z, is such that, the flux at a point "out" of the shield, either from the cylindrical source or the equivalent linear source, are of the same magnitude. The value of z to use for a particular arrangement is readily available in graphical form from data provided in shielding manuals, and it is found to be depended for photons of a certain energy E_γ on R, r, the source material (μ_s), the shielding slab

material (μ), and the slab thickness. The rest of the procedure follows the one of paragraph 2.9.2

For $r \geq 10\,R$, z is given from the graph of Fig. 2.17.

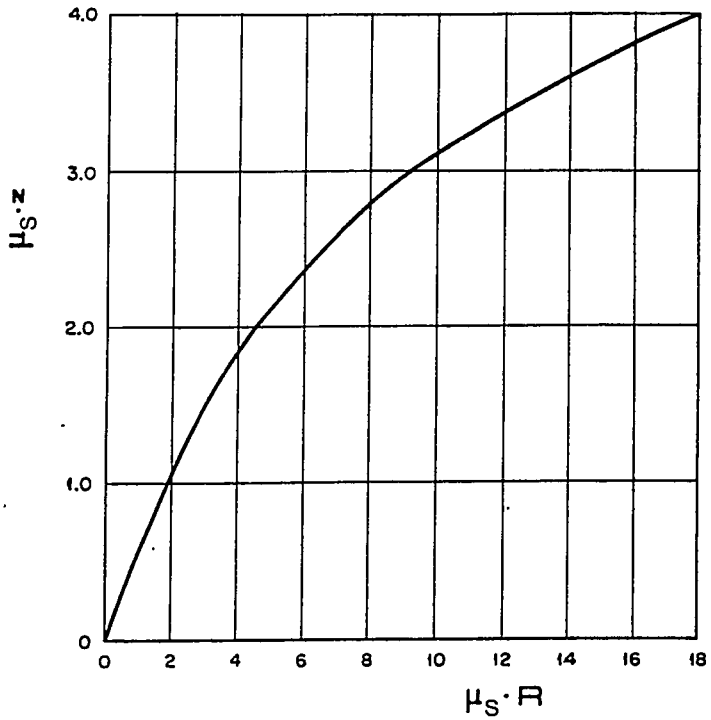

Fig. 2.17 Graph of the magnitude $\mu_s z$ as a function of $\mu_s R$ for the case where $r \geq 10\,R$.

For $r < 10\,R$, z is estimated in two steps. First we estimate from the graphs of Fig. 2.18 factor m, and then from the graphs of Fig. 2.19 the magnitude $\mu_s z/m$, hence z.

After the estimation of the self absorption distance z, we apply the procedure mentioned in paragraph 2.9.2 and we find by accepting the *Taylor's form* for the buildup factor and also that the *Blizard's method* is valid,

$$\Phi'_{P_1} = \frac{S_v \cdot R^2}{4(r+z)} \cdot \left\{ A\left[F[\vartheta_1, (1+a_1)\cdot(\mu d+\mu_s z)] + F[\vartheta_2, (1+a_1)(\mu d+\mu_s z)]\right] \right.$$

$$\left. +(1-A)\cdot\left[F[\vartheta_1, (1+a_2)(\mu d+\mu_s z)] + F[\vartheta_2, (1+a_2)\cdot(\mu d+\mu_s z)]\right] \right\} \quad (2.95)$$

For $\theta_1 = \theta_2 = \theta$, expression (2.95) gives:

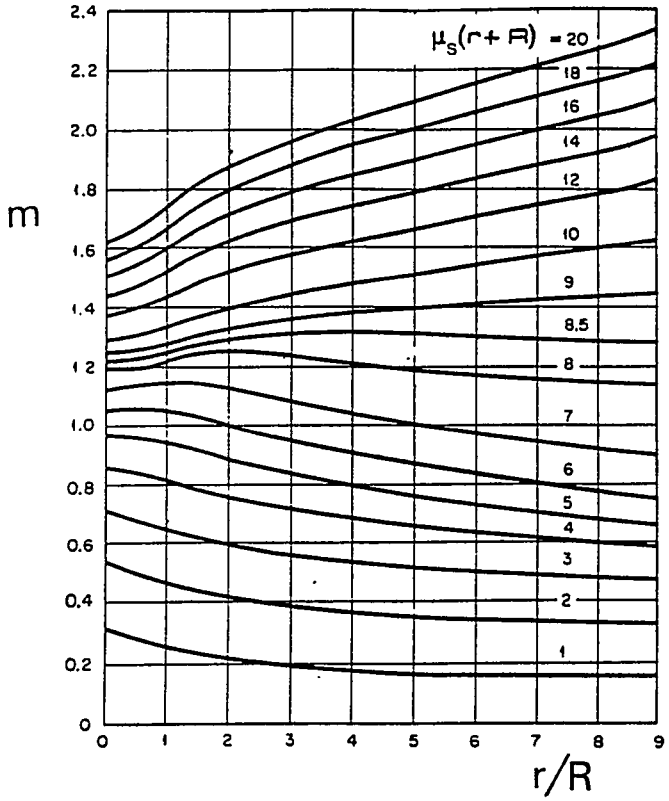

Fig. 2.18 Graphs of factor m as a function of ratio r/R, with parameter $\mu_s(r+R)$, for $r < 10\,R$.

$$\Phi'_{P_1} = \frac{S_v R^2}{2(r+z)} \cdot \left\{ A \cdot F\left[\vartheta, (1+a_1)\cdot(\mu d+\mu_s z)\right] + \right.$$

$$\left. + (1-A)\cdot F\left[\vartheta, (1+a_2)\cdot(\mu d+\mu_s z)\right] \right\} \qquad (2.96)$$

For the point P_2, we obtain,

$$\Phi'_{P_2} = \frac{S_v \cdot R^2}{4(r+z)} \cdot \left\{ A \cdot \left[F\left[\vartheta_2, (1+a_1)\cdot(\mu d+\mu_s z)\right] - F\left[\vartheta_1, (1+a_1)\cdot(\mu d+\mu_s z)\right]\right] + \right.$$

$$\left. + (1-A)\cdot\left[F\left[\vartheta_2, (1+a_2)(\mu d+\mu_s z)\right] - F\left[\vartheta_1, (1+a_2)(\mu d+\mu_s z)\right]\right] \right\} \qquad (2.97)$$

The various magnitudes in the above expressions have the usual meanings.

2.9.7 Spherical source shielded with a slab of material.

We consider the homogeneous spherical source of gamma rays, of radius R and of intensity S_V monoenergetic photons / $cm^3 \cdot sec$, shielded with a slab of material of thickness d, as is shown in Fig. 2.20.

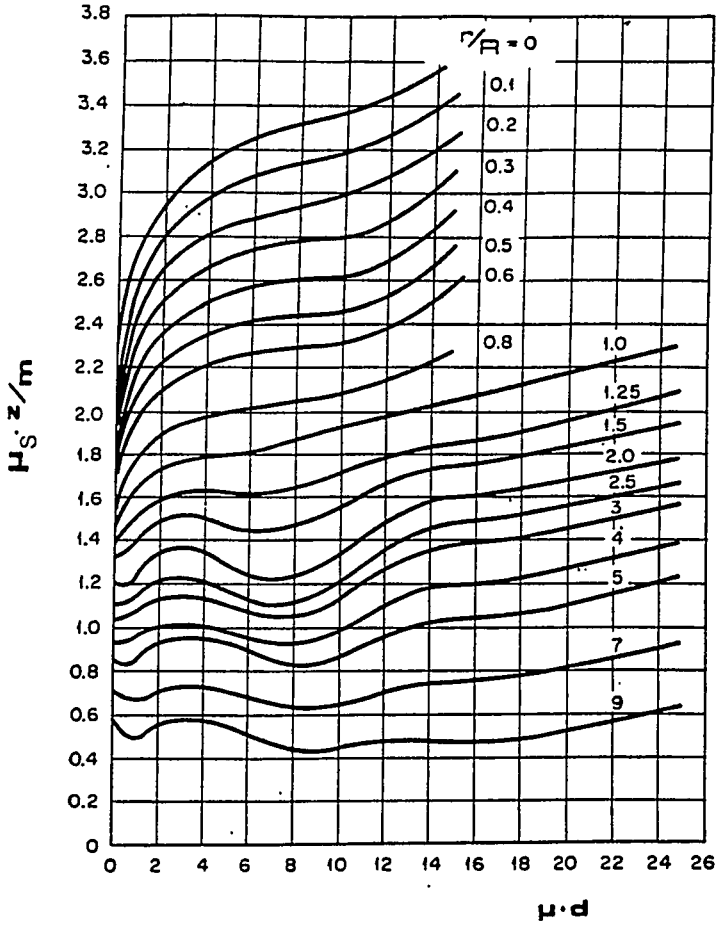

Fig. 2.19 Graphs of magnitude μ_s z/m , as a function of μ d, with parameter r/R for r < 10 R.

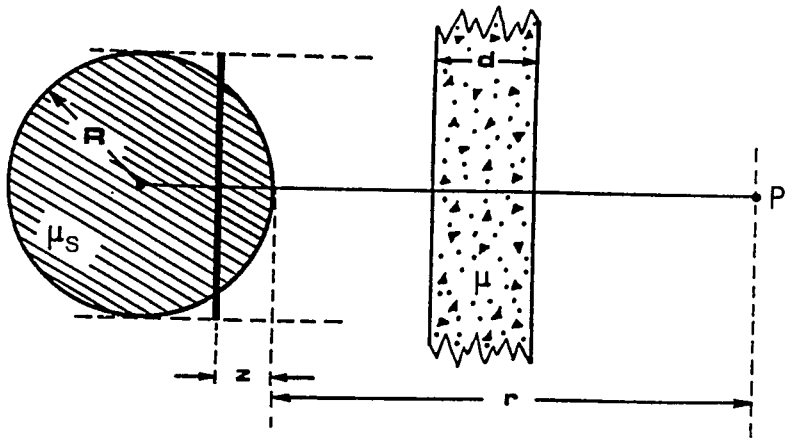

Fig. 2.20 Shielding a spherical source with a slab.

For the calculation of the buildup flux at a point P, positioned on the line drawn from the center of the spherical source perpendicularly to the slab, it is recommended to replace (as in the previous paragraph) the spherical source by an equivalent isotropic disc source whose radius equals that of the sphere. The intensity of this equivalent disc source is: $S_S = (4/3)\, R\, S_V$. The position of the disc source is determined by *the self-absorption distance z*. The value of z to use for a particular arrangement is available from graphs provided in shielding manuals and it is found to be depended for photons of a certain energy E_γ, on R, r and the source material (μ_s).

For $r \geq R$, z is estimated from Fig. 2.21, while for $r < R$, from the graphs of Fig. 2.22. After the estimation of the self absorption distance z, we apply the procedure mentioned in paragraph 2.9.3 and we find by accepting the *Taylor's form* for the buildup factor, and also that the *Blizard's method* is valid, that:

$$\Phi'_P = \frac{2}{3}\cdot S_V \cdot R\left\{A\cdot\left[E_1[(1+a_1)(\mu d+\mu_S z)] - E_1[(1+a_1)(\mu d+\mu_S z)\sec\vartheta_0]\right] + \right.$$

$$\left. + (1-A)\cdot\left[E_1[(1+a_2)(\mu d+\mu_s z)] - E_1[(1+a_2)(\mu d+\mu_s z)\sec\vartheta_0]\right]\right\} \quad (2.98)$$

Where:

$$\sec\theta_0 = \sqrt{1+\left(\frac{R}{r+z}\right)^2} \quad (2.99)$$

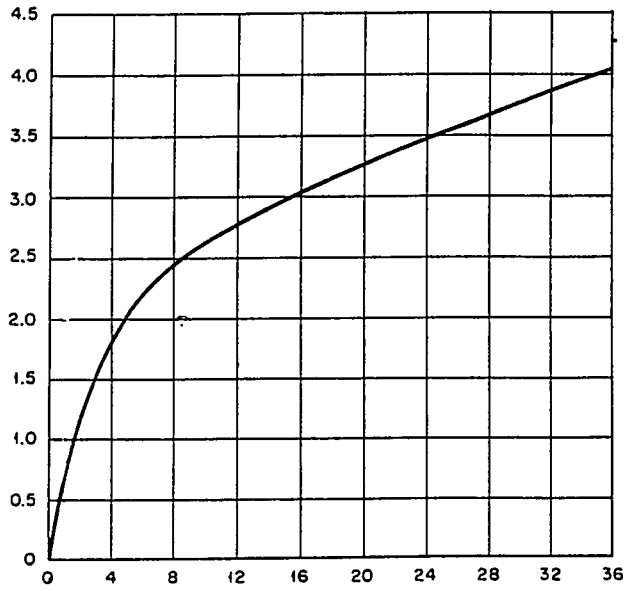

Fig. 2.21 Graph of the magnitude $\mu_s z$, as a function of $\mu_s R$, for the case of $r \geq R$.

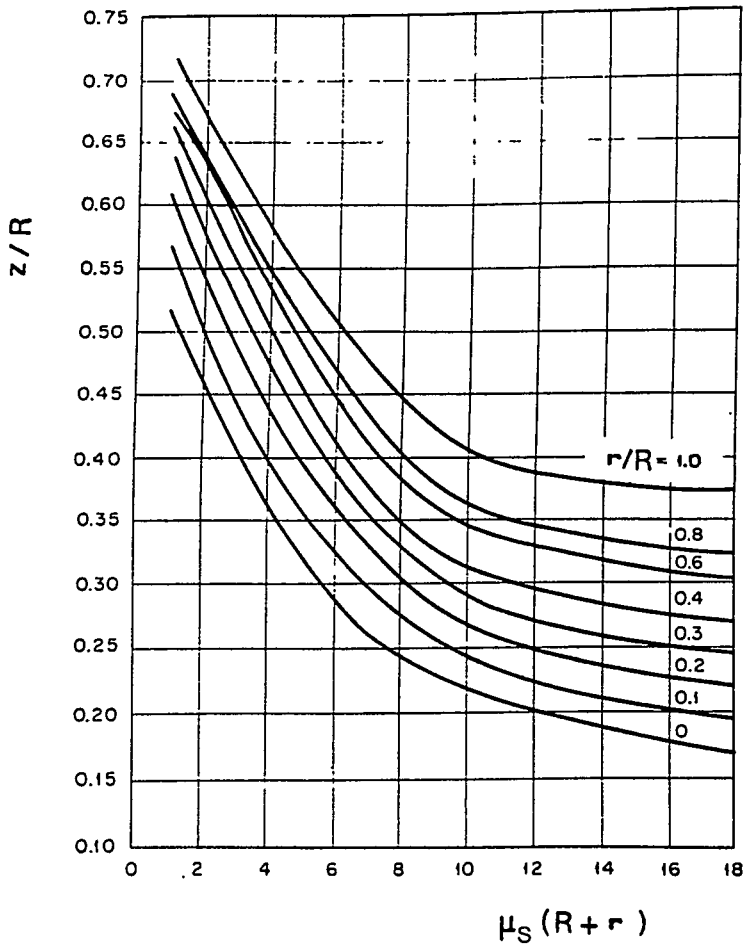

Fig. 2.22 Graphs of the ratio z/R as a function of the magnitude $\mu_s(R+r)$, with parameter r/R, for the case of $r < R$.

3. INTERACTION OF NEUTRONS WITH MATTER

In common with gamma rays, neutrons carry no charge and therefore cannot interact in matter by means of the Coulomb forces with either the orbital electrons or the nuclei. Thus, for neutrons to affect matter, they must enter the nucleus or come sufficiently close to it for the nuclear forces to act. As a result of the interaction, the neutron may either totally disappear and be replaced by one or more secondary radiations, or else, the energy or direction of the neutron is changed significantly. The possible processes of interaction are known as *neutron nuclear reactions.*

The following reactions are known:

a. Elastic scattering.
b. Inelastic scattering.
c. Radiative capture.
d. Ejection of charged particles.
e. Ejection of more than one neutrons.
f. Fission, and
g. High energy processes.

The above reactions will be analyzed in detail, in the following text, but before that, reference will be made on some basic magnitudes related with the mentioned nuclear reactions.

3.1 Nuclear cross sections.

A quantitative description of the interactions of neutrons with nuclei can be made through the use of the concepts of *nuclear cross sections.* These can be defined by the following hypothetical experiment. Suppose that a wide beam of monoenergetic neutrons impinges upon a thin target of thickness Δx and area ΔS, as shown in Fig. 3.1.

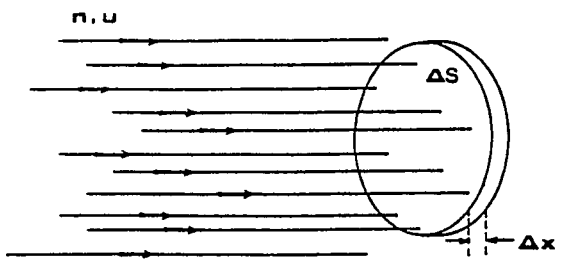

Fig. 3.1 Beam of monoenergetic neutrons striking a thin target.

If there are n neutrons per cm^3 in the beam, and υ (cm/sec) is the speed of neutrons, then the quantity,

$$I = n \cdot \upsilon \quad \text{(neutrons/cm}^2\text{·sec)} \tag{3.1}$$

is known as *the intensity of the beam*. Since the neutrons travel the distance υ cm in 1 sec, all of the neutrons existing in the volume $\upsilon \cdot \Delta S$, in front of the target will hit the target in 1 sec. Thus, $n \cdot \upsilon \cdot \Delta S = I \cdot \Delta S$ neutrons strike the entire target per second.

Since nuclei are small and the target is assumed to be thin, *most* of the neutrons striking the target in an experiment like that shown in Fig. 3.1, ordinarily pass through the target without interacting with any of the nuclei. The number of neutrons *that do collide* is found to be proportional to the beam intensity I, to the atom density N (atoms/cm^3) of the target, to the area ΔS and the thickness Δx of the target, i.e.:

$$\left\{\begin{array}{l}\text{Number of collisions}\\ \text{per second in the}\\ \text{entire target}\end{array}\right\} = \frac{dR}{dt} = \Delta R_t = \sigma \cdot I \cdot N \cdot \Delta S \cdot \Delta x \tag{3.3}$$

where σ, the proportionality constant, is called *the effective microscopic nuclear cross section.* The factor $N \cdot \Delta S \cdot \Delta x$ in equ. (3.3) represents the total number of nuclei in the target.

From equ. (3.3) we obtain:

$$\sigma = \frac{\Delta R_t}{I \cdot (N \cdot \Delta S \cdot \Delta x)} \tag{3.4}$$

from which it follows that σ is *equal to the number of collisions per sec, per nucleus* $(N \cdot \Delta S \cdot \Delta x = 1)$ *per unit intensity* $(I = 1$ *neutron/cm*^{2}*·sec) of the beam.*

There is and another way to view the concept of σ. As already mentioned, a total of $I \cdot \Delta S$ neutrons strike the target per second. Of these, $\sigma \cdot I$ interact with any given nucleus*. It may concluded therefore that:

$$\frac{\sigma I}{I \cdot \Delta S} = \frac{\sigma}{\Delta S} \tag{3.5}$$

is equal to the probability that a neutron in the beam will collide with this nucleus of the target. It is obvious from equ. (3.5) that σ has the units of area. In fact it is not difficult to see that σ is nothing more than an *effective cross-sectional area of the nucleus,* hence the term *effective microscopic nuclear cross section.*

The microscopic nuclear cross sections are expressed in units of *barns (b), millibarns (mb) and microbarns (μb),*

From equ. (3.3), for $N \cdot \Delta S \cdot \Delta x = 1$, it follows that:

$$\{\text{The number of collisions per sec per nucleus}\} = \sigma I$$

where:

$$1\ b = 10^{-24}\ cm^2$$
$$1\ mb = 10^{-27}\ cm^2$$
$$1\ \mu b = 10^{-30}\ cm^2$$

The microscopic cross section σ is a characteristic physical constant of the target nuclei, the type of nuclear reaction and depends on the neutron velocity (energy). The magnitude:

$$\Sigma = \sigma N \quad (cm^{-1}) \tag{3.6}$$

is known as *the macroscopic nuclear cross section*.

As mentioned in the begining of this chapter, neutrons ineract with nuclei in a number of ways. Each of these processes is denoted by a characteristic cross section. Thus, elastic scattering is described by the *effective elastic scattering microscopic cross section* σ_{es}, the inelastic scattering by the *effective inelastic scattering microscopic cross section* σ_{is}, the radiative capture by the *effective capture microscopic cross section* σ_{γ}, etc. The sum of the cross sections for all possible interactions with neutrons of a certain velocity, is known as *"the total effective microscopic cross section* σ_t*"*, i.e.:

$$\sigma_t = \sigma_{es} + \sigma_{is} + \sigma_{\gamma} + \ldots \tag{3.7}$$

The total effective microscopic cross section measures the probability that an interaction of any type will occur, when neutrons strike the target.

Likewise, the *"total effective macroscopic cross section"* is defined as:

$$\Sigma_t = N\cdot\sigma_{es} + N\cdot\sigma_{is} + N\cdot\sigma_{\gamma} + \ldots = N\cdot(\sigma_{es} + \sigma_{is} + \sigma_{\gamma} + \ldots) = N\cdot\sigma_t \tag{3.8}$$

The total number of neutron nuclear reactions (of any kind), taking place per cm^3, per sec, is given by analogy to equ. (3.3), by:

$$\dot{R}_t = \Sigma_t \cdot I = \Sigma_t \cdot n \cdot \upsilon \tag{3.9}$$

while the number of neutron nuclear reactions of a certain type-ν taking place per cm^3, per sec is given by:

$$\dot{R}_\nu = \Sigma_\nu \cdot n \cdot \upsilon \tag{3.10}$$

The ratio:

$$p_\nu = \frac{\dot{R}_\nu}{\dot{R}_t} = \frac{\Sigma_\nu}{\Sigma_t} = \frac{\sigma_\nu}{\sigma_t} \tag{3.11}$$

expresses *the probability that if a reaction will take place with the given nuclei and a neutron from the beam of velocity* υ*, this will be of type-*ν.

3.2 Neutron nuclear reactions.

Each of the various neutron interactions mentioned at the beginning of this chapter, may occur by way of one or more of three fundamentally different mechanisms; the *compound nucleus formation*, the *potential or shape scattering* and the *direct interaction.*

In the first process, the incident neutron is absorbed by the nucleus, and a system known as the *compound nucleus* is formed. If the target nucleus is ^{A}X, the compound nucleus is ^{A+1}X. The excitation energy of the compound nucleus includes both, the binding energy and the kinetic energy of the incident neutron. This excitation energy is distributed among the many constituents of the nucleus. The compound nucleus remains in the excited state only a short time, from 10^{-12} to 10^{-20} sec, and then the excess energy is removed by various ways leading to various results.

The potential scattering, is a type of elastic scattering, which occurs with neutrons of any energy. This mode of scattering does not involve the formation of a compound nucleus and it is similar to the scattering of one billiard ball by another. Potential scattering is only a function of the forces which act upon a neutron as it moves near the nucleus, and since these depend upon the size and shape of the nucleus, the process is also called *shape elastic scattering.*

The *direct interaction* takes place with neutrons of comparatively high energy. In this process the incident neutron collides directly with one of the nucleons, or group of nucleons in the nucleus, which then is ejected out of the nucleus.

3.2.1 The elastic scattering (n,n).

As *elastic scattering* of a neutron with a nucleus (which is considered to be initially at rest), see Fig. 3.2, is characterized the nuclear reaction in which kinetic energy and moment of the system are conserved. This interaction can take place in two ways, either by the formation of a compound nucleus, or by potential scattering. In the first case, the neutron is absorbed by the nucleus. The excitation energy brings the nucleus at a certain excitation level, from which is de-excited, ejecting a neutron and leaving the nucleus in the same internal energy situation as before the interaction.

Applying the principles of conservation of energy and momentum in the *Laboratory* and the *Center of mass* co-ordinate system, one can deduct among others, the following useful relations:

(a) Relation between the neutron kinetic energies before and after the interaction,

$$\frac{E_L'}{E_L} = \frac{A^2 + 2A\cdot\cos\vartheta + 1}{(1+A)^2} \qquad (3.12)$$

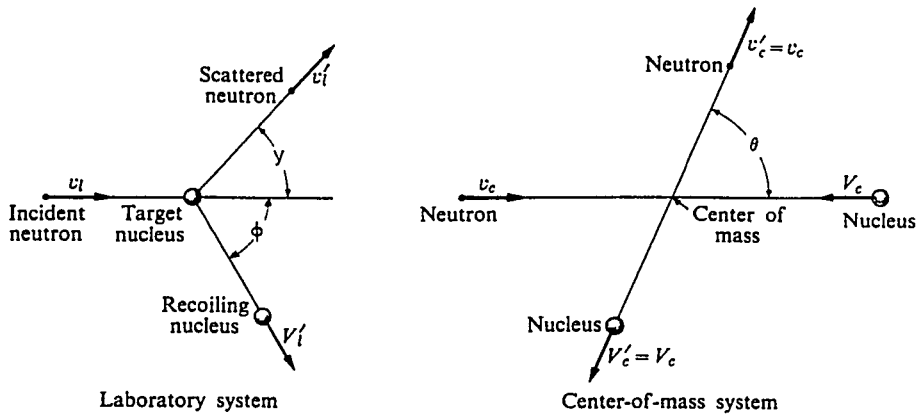

Fig. 3.2 Elastic scattering of a neutron (^{1}n) with a nucleus (^{A}X), as seen in, (a) the *laboratory* co-ordinating system (L) and (b) the *center of mass* co-ordinate system (C).

where: E_L, is the kinetic energy of the neutron before the scattering in the L-system,

E_L', is the kinetic energy of the neutron after the interaction in the L-system,

A, is the mass number of the target nucleus (A=1 for the neutron), and,

θ, is the neutron scattering angle in the C-system.

(b) Minimum neutron energy after the scattering.

From equ. (3.12), one obtains for $\theta = \pi$:

$$(E_L')_{min} = E_L \cdot \left(\frac{A-1}{A+1}\right)^2 \qquad (3.13)$$

(c) Relation between the neutron scattering angles θ and y in the two systems.

$$\tan y = \frac{\sin\theta}{1/A + \cos\theta} \qquad (3.14)$$

or,

$$\cos y = \frac{1 + A\cdot\cos\theta}{\sqrt{A^2 + 2A\cdot\cos\theta + 1}} \qquad (3.15)$$

(d) Mean value energy of the neutron after scattering.

$$\overline{E_L'} = \frac{E_L}{2}\cdot\left[1 + \left(\frac{A-1}{A+1}\right)^2\right] \qquad (3.16)$$

(e) Relation between the total kinetic energy of the system neutron-nucleus in the two co-ordinate systems.

$$E_C = \frac{A}{A+1} \cdot E_L \qquad (3.17)$$

where E_C is the total kinetic energy of the neutron and the nucleus before interaction in the C-system.

(f) Mean value of cosy.

$$\bar{\mu} = \overline{\cos y} = \frac{2}{3A} \qquad (3.18)$$

It is observed from equ. (3.14) that with increasing A, (A >>1), the difference between angles y and θ is diminished, while from equ. (3.18), that with increasing A, $\bar{\mu} \to 0$, which means that, the case of the elastic scattering of the neutron in the laboratory system may be considered spherically symmetric.

The elastic scattering microscopic cross section σ_{es} as a function of the energy of the incident neutron can be devided into three distinct regions. In the first, lower-energy region, σ_{es} is approximately constant. The scattering in this region does not occur by compound nucleus formation, but merely because of the forces, exerted by the target nucleus on the passing neutron. The microscopic cross section for this potential scattering is given by:

$$\sigma_{es} = 4\pi \cdot R^2 \qquad (3.19)$$

where, R is the *nuclear radius*.

Beyond the potential scattering region, there is a region of resonances, which is refered to compound nucleus formation. At still higher energies, the resonances crowd together to such an extent, that the individual resonances can no longer be resolved, and in this region σ_{es} is a smooth and slowly varying function of energy. Figure (3.3), shows these three regions for ^{12}C, as target nucleus. Carbon-12 is a relatively light nucleus. With heavier nuclei, the region of resonances is found at lower energies. For example, the resonance region for ^{238}U, begins at only 6 eV and ends at roughly 1 keV.

3.2.2 The inelastic scattering (n,n′).

As *inelastic scattering* of a neutron, is characterized the process in which the impinging neutron enters in the nucleus, the compound nucleus formed is excited and then de-excited ejecting a neutron, but the rest nucleus remains excited.

This process does not occur unless the neutron has sufficient energy to place the target nucleus in its first excited state. As a result, σ_{is} is zero up to some threshold energy.

Consider the collision of the neutron with the nucleus as viewed in the center

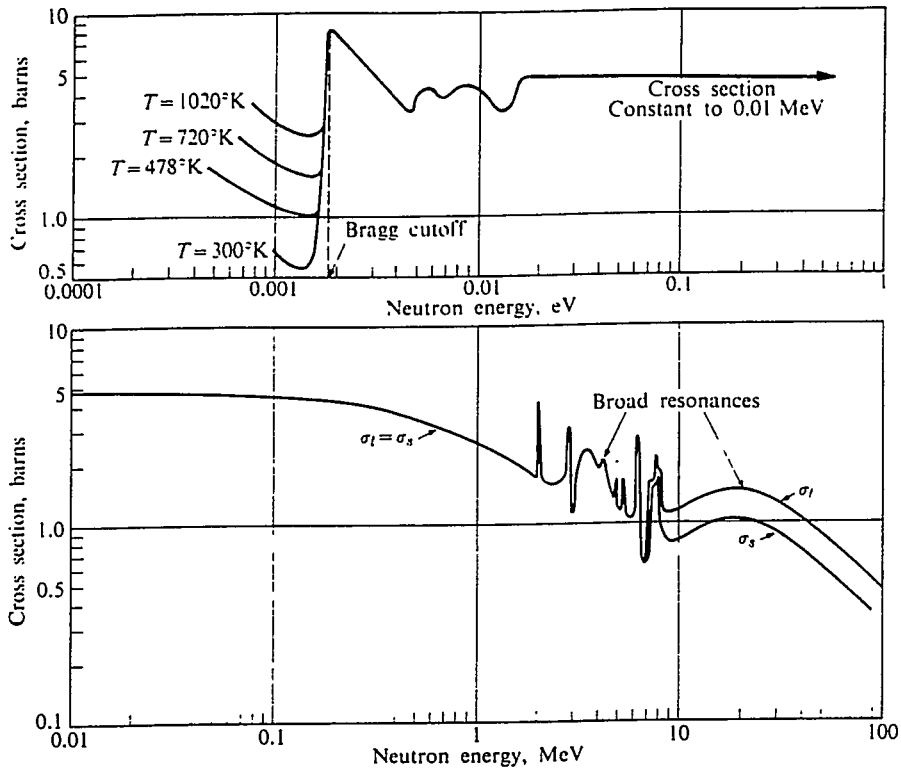

Fig.3.3 The elastic scattering and the total microscopic cross section of the ^{12}C nucleus.

of mass system (Fig. 3.2b). In this system, the two particles are seen to approach each other and collide at the center of mass. The sum of the kinetic energies of the two particles in the C-system is available to induce a reaction. If their total kinetic energy is greater than E_1, the energy of the first excited state, this state can be excited in the collision; that is, *inelastic scattering* can occur.

According to equ. (3.17) if $E_C \geq E_1$, the neutron kinetic energy in the L-system should be at least ($E_C = E_1$):

$$E_{thr} = \frac{A+1}{A} \cdot E_1 \qquad (3.20)$$

The energy E_{thr} is known as the *inelastic threshold energy*, and as is shown, is always greater [given that $(A+1)/A > 1$] than the energy of the first excited state. For example, the first excited state of ^{12}C is at 4.43 MeV, but inelastic scattering to occur, the neutron kinetic energy in the L-system should be at least, $(13/12)\times 4.43 = 4.80$ MeV.

Figure 3.4 shows the microscopic inelastic scattering cross section for the excitation of the first three levels in ^{238}U, along with the total inelastic cross

section.

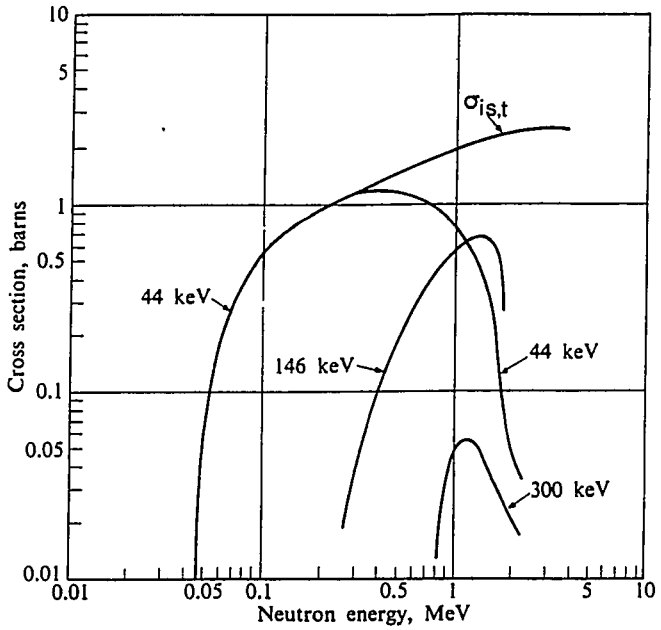

Fig. 3.4 The microscopic cross sections for the excitation of the 44 keV, 146 keV, and 300 keV levels and the total inelastic cross section of ^{238}U.

The energy at which the first excited state is found, decreases with increasing mass number, and, as consequence, σ_{is} is nonzero over a larger energy region for the heavier nuclei than for the lighter nuclei (4.80 MeV for ^{12}C, while it is only 44 keV for ^{238}U). At energies well above threshold, $\sigma_{is} \simeq \sigma_{es}$.

Inelastic scattering plays an important role in the slowing down process, of fast neutrons, either in thermal reactors, or in the shieldings, because fast neutrons reduce their energy below the threshold energy of the target nucleus. Values for inelastic scattering threshold energies, are given in Table 3.1 for various nuclei.

Table 3.1 Threshold energy values for inelastic scattering, for various nuclei.

Target nucleus	A	E_l (keV)	E_{thr} (keV)
C-12	12	4440	4810
O-16	16	6130	6513
Be-9	9	1700	1889
Fe-56	56	845	860
Th-232	232	50	50.2
U-238	238	45	45.2

3.2.3 The radiative capture (n,γ).

As radiative capture is characterized the process in which the neutron enters the nucleus, and the excited compound nucleus de-excite by emission of γ-radiation. This process can occur at all neutron energies, but it is most probable at low energies, and in particular at those energies that lead to *long-lived* states of the compound nucleus.

Since the excitation level of the compound nucleus is above the virtual energy, the system can decay also by the re-emission of a neutron. It is observed that radiative capture is comparatively unimportant in light nuclei, but becomes increasingly important in the heavier nuclei.

In Fig. 3.5 is shown the microscopic radiative capture cross section σ_γ for ^{197}Au. A strong peak appears at the first resonance ($E_1 \simeq 5$ eV), while at lower neutron energies, a 1/υ behaviour is observed.

Breit and *Wigner* give the following expression for σ_γ near an isolated resonance:

$$\sigma_\gamma(E_C) = \sigma_0 \cdot \left(\frac{E_1}{E_C}\right)^{1/2} \cdot \frac{\Gamma_n \cdot \Gamma_\gamma}{(E_C - E_1)^2 + \Gamma^2/4} \qquad (3.21)$$

where: E_C , is the total kinetic energy of the incident neutron and the target nucleus, with respect to the center of mass co-ordinate system,
E_1 , is the first resonance energy of the compound nucleus,
σ_0 , is a constant, and
Γ_n, Γ_γ , *the neutron radiation widths,* while
$\Gamma = \Gamma_n + \Gamma_\gamma$.

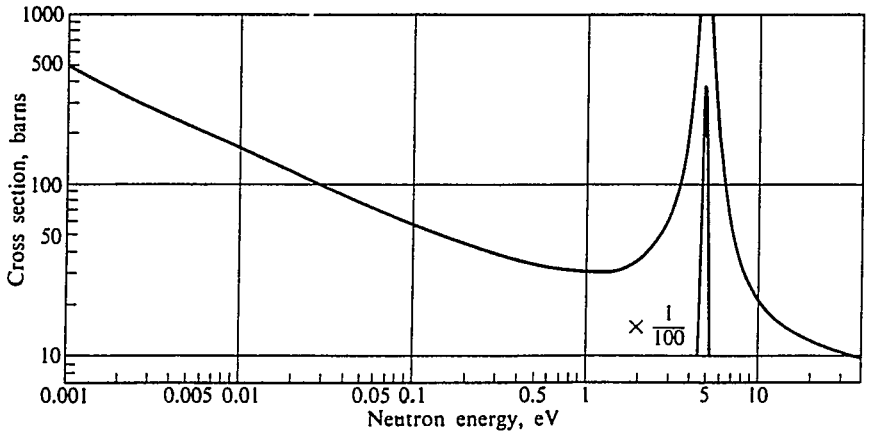

Fig. 3.5 The total radiative capture microscopic cross section of ^{197}Au .

It may be observed that when the target nucleus is heavy enough, we may consider (see paragraph 3.2.1) that $E = E_L \simeq E_C$, and if E_C is $<< E_1$, equation (3.21) gives:

$$\sigma_\gamma \simeq \sigma_0 \cdot \frac{\Gamma_n \cdot \Gamma_\gamma}{E_1^2 + (\Gamma/2)^2} \cdot \sqrt{\frac{E_1}{E}} \qquad (3.22)$$

i.e.: $$\sigma_\gamma \sim 1/\sqrt{E} \sim 1/\upsilon \qquad (3.23)$$

as is observed in Fig. 3.5 for $E << 5$ eV.

For energies E: $E >> E_1$, it is found that σ_γ is diminished with increasing energy according to the law 1/E or faster. For example, for ^{238}U, is $\sigma_\gamma \sim 1/E^\alpha$ where $\alpha = 1.1 \div 1.6$.

3.2.4 Ejection of charged particles (n,p), (n,α).

Sometimes, if the impinging neutron kinetic energy is adequate, the compound nucleus ejects a proton (n,p), or a group of nucleons like an alpha particle (n,α). As a rule, the (n,p), (n,α) and other possible charged-particle reactions, are *endothermic* and do not occur below some threshold energy. Their cross sections also tend to be small, even above threshold energies, especially for the heavier nuclei.

However, there are some important *exothermic* reactions in light nuclei. One of these, is the reaction $^{10}B(n,\alpha)\,^7Li$, the microscopic cross section of which is shown in Fig. 3.6. It is observed that σ_α is very large at low neutron energies, and for this reason B-10 is often used to absorb low energy neutrons. The 1/υ behaviour is obvious.

A similar exothermic reaction which also shows a strong 1/υ behaviour is the $^6Li(n,\alpha)\,^3H$. This reaction is used for the production of tritium (H-3).

Some endothermic charged particle reactions are important in reactors, even though their thresholds are high. In water reactors, for example, the $^{16}O(n,p)\,^{16}N$ reaction is the principal source of the radioactivity of the water. The N-14 undergoes β-decay, with a half-life of approximately 7sec, which is accompanied by the emission of 6 to 7 MeV γ-rays. The threshold for this reaction is 9 MeV and as a consequence only about one neutron in several thousand, has the suitable energy for this to happen.

3.2.5 Ejection of more than one neutrons (n,2n), (n,3n).

The (n,2n) reaction usually proceeds in two steps:

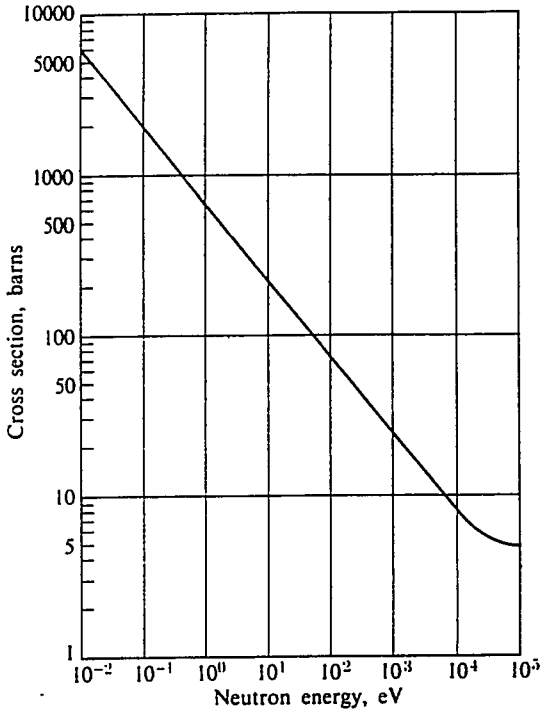

Fig. 3.6 The microscopic cross section for the $^{10}B(n,\alpha)\,^{7}Li$ reaction, from 0.01 eV to 10^5 eV.

First, the incident neutron is inelastically scattered by the target nucleus. Then, if the residual nucleus is left with an excitation energy above the binding energy of its least bound neutron, this neutron is possible to escape from the nucleus.

In order that the reaction (n,2n) will take place, the incident neutron energy should be above the threshold energy of this reaction. This energy is given in the L-system, by:

$$E_{thr} = \frac{A+1}{A} \cdot Q \qquad (3.24)$$

where Q is the *Q-value of the (n,2n) reaction.*

One of the most important examples of this kind is ^{9}Be, whose (n,2n) threshold is only 1.8 MeV. With most nuclei, however, the (n,2n) threshold is in the range of $7 \div 10$ MeV.

The relationship of the (n,3n) reaction to the (n,2n) reaction is similar to that of (n,2n) reaction to inelastic scattering. Thus, a third neutron will be emitted, provided the nucleus retains sufficient excitation energy after the emission of the second neutron in the (n,2n) reaction.
In Fig. 3.7 are shown the microscopic cross sections for the (n,n), (n,2n) and (n,3n) reactions, for the ^{238}U nucleus.

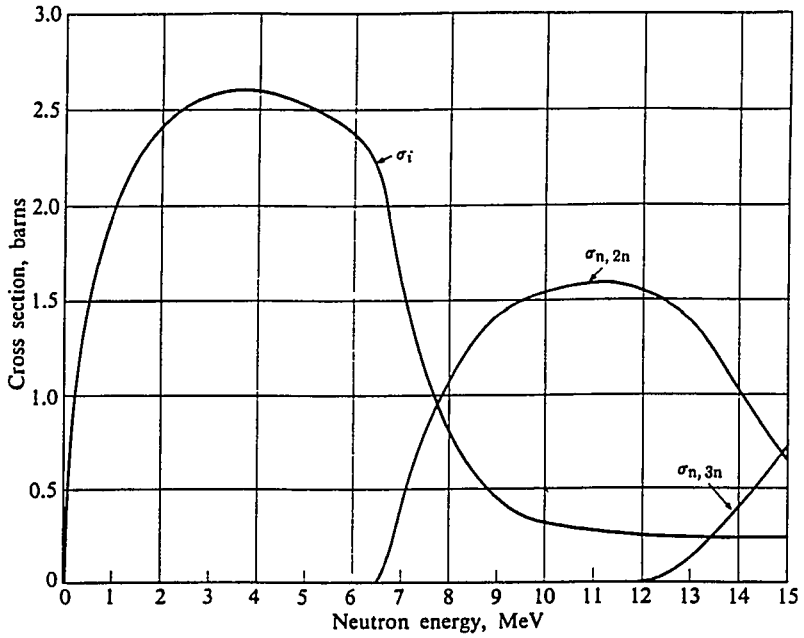

Fig. 3.7 The inelastic, (n,2n), and (n,3n) microscopic cross of ^{238}U.

The (n,3n) thresholds are usually so high (they range from about 11 MeV to 30 MeV), that these reactions are rare. It may be mentioned that if a nucleus has a low (n,2n) threshold, it does not necessarily follow that its (n,3n) threshold will also be low. For instance, the threshold for the ^{9}Be, (n,3n) reaction is 21 MeV.

The origin of this disparity lies in the fact that although it may require only a small amount of energy to remove one neutron from a nucleus, it may take considerably more energy to remove a second one.

3.2.6 Fission of the heavy nuclei.

Nuclear fission is the process in which a heavy nucleus splits into two fragments, with the release of considerable energy (~ 200 MeV) and the emission of neutrons, neutrinos and γ-rays, as is shown in Fig. 3.8.
The fission process usually takes place when a neutron of adequate energy (from 0 to about 1.3 MeV), hits a heavy nuclei, but it is also possible to take place spontaneously or if the nucleus is exposed to γ-rays of energy above the known as *critical energy* (4.0 MeV to 6.5 MeV).

In Table 3.2 are given the heavy nuclei which can undergo fission by neutrons, together with the neutron threshold energies, while in Table 3.3 are given the critical energies of the fissioning nuclei.

From Table 3.2, is shown that for some heavy nuclei the neutron threshold energy $E_{thr.f}$ is zero. These nuclei (^{234}U, ^{235}U, ^{239}Pu and ^{241}Pu) are known as

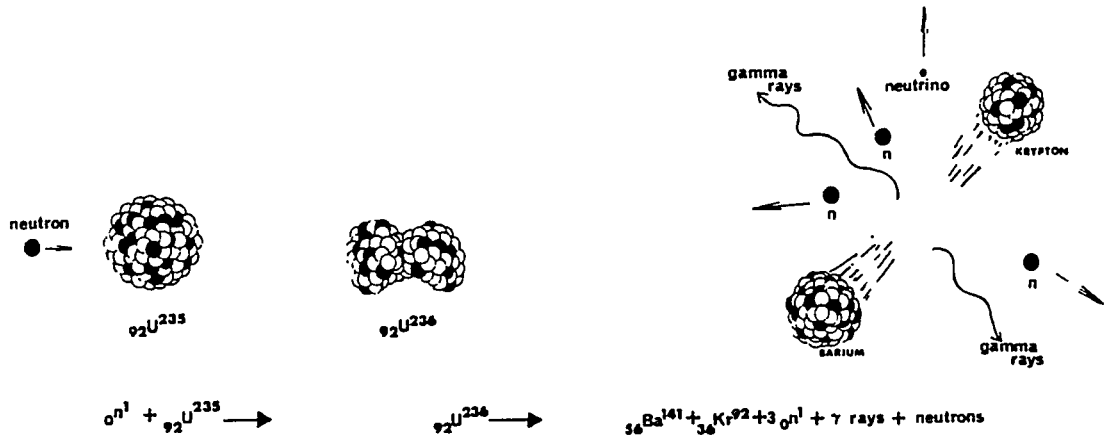

Fig. 3.8 An example of the fission process.

Table 3.2 Threshold neutron energies for the heavy nuclei.

Nuclei-target	Compound nuclei	$E_{thr,f}$ (MeV)	$\nu_{thr.f}$
Th-232	Th-233	1.3	2.1
U-233	U-234	0.0	2.5
U-234	U-235	0.4	-
U-235	U-236	0.0	2.4
U-236	U-237	0.8	-
U-238	U-239	1.2	2.5
Np-237	Np-238	0.4	-
Pu-239	Pu-240	0.0	2.9
Pu-241	Pu-242	0.0	3.0

Table 3.3 Critical energies for fission of heavy nuclei.

Fissioning nucleus ^AZ	**Critical energy**	**Binding energy of last neutron in ^AZ**
^{232}Th	5.9	*
^{233}Th	6.5	5.1
^{233}U	5.5	*
^{234}U	4.6	6.6
^{235}U	5.75	*
^{236}U	5.3	6.4
^{238}U	5.85	*
^{239}U	5.5	4.9
^{239}Pu	5.5	*
^{240}Pu	4.0	6.4

*Neutron binding energies are not relevant for these nuclei since they cannot be formed by the absorption of neutrons by the nuclei ^{A-1}Z.

fissile nuclei, while those for which $E_{thr,f} > 0$ are known as *fissionable nuclei* (^{232}Th, ^{234}U, ^{236}U, ^{238}U, ^{237}Np).

In Fig. 1.4 are given the fission yields as a function of mass number of ^{235}U, for thermal and 14 MeV neutrons. In these curves the ordinate (yield, %) is the probability expressed in percent, that a fission fragment of a given mass number is produced in fission. It is obvious that fission, almost always, occurs in an asymmetric fashion, and that symmetric fission is, in fact, a comparatively *rare event.*

The average number of neutrons, released per fission is given the symbol ν. In Table 3.2 (last column) are given the values for $\nu_{thr,f}$, corresponding to the threshold fission neutron energies.

Since the absorption of a low-energy neutron by a fissile nucleus does not always lead to fission (de-excitation of the compound nucleus by the emission of γ-ray), a parameter (η) is introduced, which is *equal to the average number of neutrons emitted in fission per neutron absorbed in the fissile isotope.* This quantity (η) is equal to ν times the relative probability that a neutron absorption by a heavy nucleus, leads to fission; thus:

$$\eta = \nu(\sigma_f/\sigma_\alpha) \tag{3.25}$$

or,

$$\eta = \nu/(1+\alpha) \tag{3.26}$$

where: σ_f , is the microscopic cross section for fission,
$\sigma_\alpha = \sigma_f + \sigma_\gamma$, is the microscopic absorption cross section,
σ_γ , is the microscopic cross section for radiative capture, and
$\alpha = \sigma_\gamma / \sigma_f$, is the *capture to fission ratio.*

The fission neutrons emitted promptly (i.e., within about 10^{-17} sec of the fission event), follow a continuous energy distribution (Fig. 3.9). This distribution is described by the function $\chi(E)$, which is called *the prompt-neutron spectrum.*
This is defined so that $\chi(E)\,dE$ denotes the number of neutrons emitted with *laboratory energie* between E and E+dE *per fission neutron*, that is, $\chi(E)$ is normalized so that,

$$\int_0^\infty \chi(E)\,dE = 1 \tag{3.27}$$

One recent expression, given in the literature for the neutron spectrum is the following:

$$\chi(E) = 0.453 \cdot e^{-1.036\,E} \sinh\sqrt{2.29\,E} \tag{3.28}$$

where E in MeV.

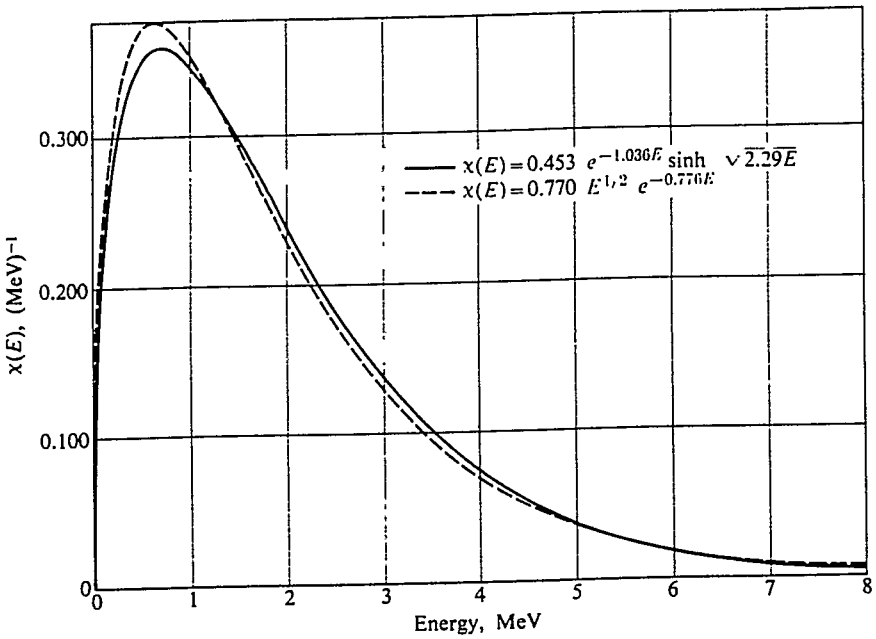

Fig. 3.9 The prompt neutron spectrum computed from the mentioned (in the figure) two expressions.

It is easily found from equ. (3.28) that the *mean energy* $\overline{E}$ of the prompt neutrons is:

$$\overline{E} = \int_0^\infty E \cdot \chi(E)\, dE = 1.98 \text{ MeV} \qquad (3.29)$$

while, the *most probable* neutron energy, that is, *the energy corresponding to the peak of the* $\chi(E)$ *curve,* is only about 0.73 MeV.

3.2.7 High – energy processes.

The capture in nuclei of neutrons with high energies, above 50 MeV, may cause the emission of a shower of many different types of particles. The process is known also as *spallation*. At energies of 100 MeV or more, a dozen or more nucleons may escape and many combinations of protons and neutrons are observed. The theory of the compound nucleus does not apply to these reactions because there is not enough time for the excitation energy to be shared among all the nucleons before particles start being emitted. The further discussion is beyond the scope of these lectures, since it belongs in the field of high energy nuclear physics.

3.3 Neutron attenuation.

Consider a monodirectional beam of monoenergetic neutrons, of intensity I_0 (neutrons/cm^2·sec), incident upon a slab of material, of thickness d, as shown in Fig. 3.10. If N indicates the number of the target nuclei per cm^3, and I(x) is the intensity of the beam (composed of non-interacted neutrons) in depth x, then the decrease of I(x) for an increment of x by dx will be dI(x). This decrement, due to the number of neutrons that have interacted in the thin sheet of thickness dx, is proportional to I(x), N and dx, i.e.,

$$-dI(x) = \sigma_t \cdot N \cdot I(x) \cdot dx \qquad (3.30)$$

according to equation (3.4).

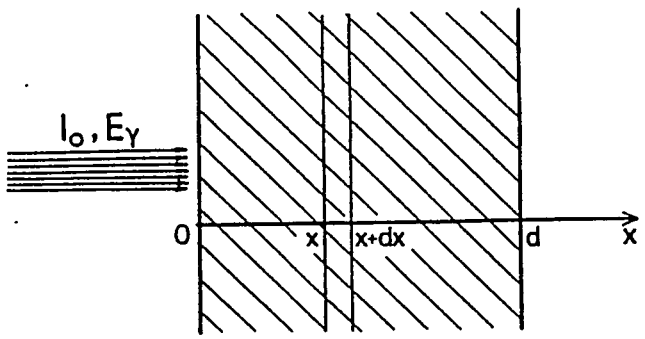

Fig. 3.10 Attenuation of a collimated monoenergetic neutron beam.

The total microscopic cross section σ_t is used in equ. (3.30), because by definition *any interaction removes a neutron from the noninteracted since then, neutrons of the beam.* The "-" sign in the differential equation (3.30) indicates that the intensity of the beam decreases with increasing x (i.e., with positive dx).
The solution of equation (3.30), with initial condition that: $I(0) = I_0$ for x=0, gives:

$$I(x) = I_0 \, e^{-\sigma_t \cdot N x} = I_0 \, e^{-\Sigma_t \cdot x} \qquad (3.31)$$

given that: $\Sigma_t = \sigma_t \cdot N$, the macroscopic total cross section.

From equ. (3.31) one obtains:

$$p(x) = \frac{I(x)}{I_o} = e^{-\Sigma_t \cdot x} \qquad (3.32)$$

which denotes *the probability that a neutron can move through the distance 0÷x without interacting with the nuclei of the slab.*

From equ. (3.30) one obtains:

$$p'(x)\cdot dx = \left|\frac{d\,I(x)}{I(x)}\right| = \Sigma_t \cdot dx \qquad (3.33)$$

which denotes *the probability that the neutron being at depth x, will interact between x and x+dx.*

The product of the above two probabilities,

$$P(x)\cdot dx = p(x)\cdot p'(x)\cdot dx = e^{-\Sigma_t \cdot x}\cdot \Sigma_t \cdot dx \qquad (3.34)$$

gives *the probability, a neutron of the initial beam, to reach depth x without any interaction and then to have a collision between x and x+dx.* By analogy, the probability P(a,b) *that a neutron will have its first interaction between x=a and x=b, is simply the integral of P(x)·dx between these limits.* That is:

$$P(a,b) = \Sigma_t \cdot \int_a^b e^{-\Sigma_t \cdot x}\cdot dx = e^{-\Sigma_t a} - e^{-\Sigma_t b} \qquad (3.35)$$

In particular, *the probability that a neutron will interact at least once in an infinite medium is obtained by placing a=0 and b=∞*, thus:

$$P(0,\infty) = \int_0^\infty P(x)\cdot dx = 1 \qquad (3.36)$$

as would be expected.

The distance that a neutron moves between interactions, is called *a free path*, and the average distance between interactions is known as the *mean free path.* This quantity, which is designated by the symbol λ (not to be confused with the radioactive decay constant) is given by:

$$\lambda = \int_0^\infty x\cdot P(x)\cdot dx = \Sigma_t \cdot \int_0^\infty x\cdot e^{-\Sigma_t x}\cdot dx = 1/\Sigma_t \qquad (3.37)$$

The intensity of the beam emerging from the slab is according to equ. (3.31):

$$I(d) = I_0 \cdot e^{-\Sigma_t d} \qquad (3.38)$$

3.4 Neutron activation.

When a target of nuclei is exposed in a beam of monoenergetic neutrons, some of the nuclei capture neutrons and the compound nuclei decay or de-excite by various processes, emitting thus charged particles (p,α) or γ-rays.

The decay follows the fundamental law of radioactivity, namely, that *the probability per unit time that a nucleus decays is a constant independent of time.*

This constant is called *the decay constant*, is denoted by λ, and is characteristic of the decaying nucleus.
The radioactivity law is expressed as follows:

$$N(t) = N_0 \cdot e^{-\lambda \cdot t} \tag{3.39}$$

where: N_0, is the number of radioactive nuclei existing at t=0.

If, a target of a certain kind of nuclei is exposed to a beam of neutrons, of constant intensity I, the rate of change of the number of radioactive nuclei will be the difference between the *rate of production,*

$$\dot{R} = \sigma \cdot n_0 \cdot I \tag{3.40}$$

where: σ is the microscopic cross section for the capture of neutrons by the target nuclei, and
n_0 is the amount of the target nuclei considered (in a first approach) constant during the exposure in the neutron beam,

and the *rate of decay* P(t) of the compound radioactive nuclei:

$$\dot{P}(t) = \lambda \cdot n(t) \tag{3.41}$$

where: n(t), is the number of radioactive nuclei existing at time t.

Thus, the differential equation describing the change with time of the radioactive nuclei, is:

$$\frac{dn(t)}{dt} = \text{(production rate) - (decay rate)}$$

or,

$$= \dot{R} - \dot{P}(t) = \dot{R} - \lambda \cdot n(t) \tag{3.42}$$

$\dot{R}$, is assumed to be a constant, because we may neglect the small decrease in the number of stable atoms n_0, which remain to be exposed for activation.

With initial condition, that at t=0, n(0)=0, the solution of the above equation (3.42) is:

$$n(t) = \frac{\dot{R}}{\lambda} \cdot (1 - e^{-\lambda t}) \quad , \quad t: \ 0 \leq t \leq t_0 \tag{3.43}$$

and the radioactivity $\dot{P}_1(t)$ of the target during the activation process:

$$\dot{P}_1(t) = \dot{P}(t) = \lambda \cdot n(t) = \dot{R} \cdot (1 - e^{-\lambda t}) \tag{3.44}$$

The radioactivity of the target at the end of activation (t_0) will be:

$$\dot{P}_{1,0} = \dot{P}_1(t_0) = \dot{R} \cdot (1 - e^{-\lambda t_0}) \tag{3.45}$$

For t_0 : $t_0 >> 1/\lambda = \tau$ ($\tau = 1/\lambda$, the mean life time of the radioactive nuclei), the radioactivity of the target tends to the constant value:

$$\dot{P}_s = \dot{R} \tag{3.46}$$

the known as *saturation activity*, which according to equ. (3.45) is equal to the production rate of the radioactive nuclei.

After time t_0 (i.e., for t : $t > t_0$), the target decays according to the law (3.39), and its radioactivity is given by :

$$\dot{P}_2(t) = \dot{P}_{1,0} \cdot e^{-\lambda(t-t_0)} = \dot{R} \cdot (1 - e^{-\lambda t_0}) \cdot e^{-\lambda(t-t_0)} \tag{3.47}$$

The situation during and after the exposure of the target to the beam of neutrons, is depicted in Fig. 3.11 .

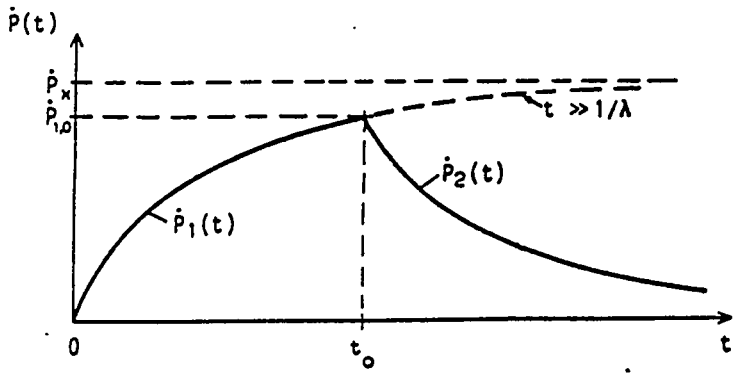

Fig. 3.11 Radioactivity of a specimen of nuclei exposed to a neutron beam for time t : $0 \leq t \leq t_0$.

By using equations (3.47) and (3.40) , it is possible through experimentally measured magnitudes and known constants (σ, λ, n_0) , to deduce the intensity of the neutron beam, in which the target was exposed.

3.5 Shielding of neutron sources .

By far the greatest neutron source is the operating reactor, in which, along with the prompt gamma rays, free neutrons are released as part of the fission event. However, other reactions can also produce neutron sources of importance to the shield designer.

3.5.1 General considerations.

The fission as a neutron source has been described in paragraph 3.2.6. It has been mentioned that the prompt neutrons produced during fission are characterized by a continuous energy spectrum, which extends from zero energy (eV region) to beyond 18 MeV. The average energy of fission neutrons is about 2 MeV. Except the prompt fission neutrons, there are several other sources of radiation to be considered in a fission reactor; these are the following:

There are *delayed fission neutrons,* i.e. neutrons that are emitted from some fission products (the known as *delayed neutron precursors*) with a time delay relative to the fission event in which they were produced. Ordinarily these are not of important consideration because, on the one hand, there are so few of them, and on the other hand, their energies are so low (on the order of 400 keV). Delayed neutrons can, however, lead to special shielding problems in *circulating fuel reactors* like the *molten salt breeder reactor.* In that system, the delayed neutron precursors are carried outside of the core with the moving fuel, and some of the delayed neutrons are emitted there.

There are *fission* γ*-rays*, i.e. γ-rays emitted in the core during the fission processes, and also *fission product decay* γ*-rays.* These γ-rays is a continuing source of radiation and after the shutdown of a reactor, due to the fission fragments accumulated in the fuel elements.

There are γ-rays emitted by the nuclei which have been left in excited states as the result of inelastic neutron scattering. Since inelastic scattering occurs only with energetic neutrons, the inelastic γ-rays tend to be emitted from the reactor core and from inner portions of the shield where the neutrons are most energetic.

There are capture γ-rays, i.e. γ-rays emitted each time a neutron is absorbed by a nucleus in a radiative capture reaction. This reaction is most probable at resonance and thermal energies. Since thermal neutrons are usually present in a reactor shield, the shield itself may be a source of capture γ-rays. Also much of the internal structure of the reactor becomes γ-radioactive in this way, and so does the coolant and any extraneous atoms contained in the coolant. Such radionuclides, contained in, or picked up and carried along by the coolant may be deposited along the piping and equipment located in the primary coolant loop, so that these parts become sources of γ-rays that require shielding.

Practically it is found that among all of these radiation sources, the prompt fission neutrons are the most difficult to shield against; and this because it is not possible to absorb fast neutrons, due to the *too small microscopic absorption cross sections at high energies.* To face this problem, it is necessary first to slow down the fast neutrons to thermal energies, and then

absorb the so-formed thermal neutrons. It should be reminded here that neutrons loose 50 % of their energy, on average, in elastic collisions with hydrogen nuclei, more than with any other nucleus. This is the reason that hydrogen is pursued to be one of the principal components of the neutron shields. Water, with its high hydrogen content, as well as other materials containing water are often employed to shield strong neutron sources like reactor installations.

Most of the shielding in stationary nuclear power plants is concrete with special additives. Concrete contains approximately 10 % per weight water and has a hydrogen atom density ($1.4 \cdot 10^{22}$ nuclei/cm^3) equal to about 1/4 that of the water itself ($6.7 \cdot 10^{22}$ nuclei/cm^3). Concrete is inexpensive, structurally sound, and can readily be formed into any desired shape, monolithic or brick shape.

Some special types of concrete contain moderately heavy or heavy materials to slow down the neutrons by inelastic collisions. Such nuclei are found in the following additives:

- Limonite ($2Fe_2O_3 \cdot 3H_2O$)
- Barytes mineral
- Colemanite ($Ca_2B_6O_{11} \cdot 5H_2O$)

Iron has been used extensively, either in solid sheets or distributed uniformly in concrete, but more for the purpose of attenuating γ-rays.

The absorption of the thermalized neutrons is the last scope of the neutron shield. However, when thermal neutrons are absorbed by hydrogen nuclei, a 2.2 MeV γ-ray is emitted as the result of the $^1H(n,\gamma)^2H$ reaction. If they are captured by iron, a 7.6 MeV and a 9.3 MeV γ-ray are emitted. The exposure rates from these γ-rays outside the shield can be quite significant, especially if the shield is not so thick. To reduce the intensity of such γ-rays, boron, in one form or another, is added to the shielding material. Boron has a high thermal absorption cross section (see Fig. 3.6) for the reaction $^{10}B(n,\alpha)^7Li$, while the γ-rays accompanying this reaction are of relatively low energy (about 0.5 MeV).

Other sources of neutrons which one finds in laboratories and which need to be shielded, are sources of the *static type* like the Sb-Be, Po-Be, Pu-Be, Am-Be etc., and also the neutron generators. In the first case γ-rays (from Sb), or α-particles (from Po, Pu and Am) cause reactions of the (γ,n) or (α,n) type. In the second case neutrons are produced according to the reaction $^3H(d,n)^4He$.

3.5.2 Removal theory.

From a series of experiments, carried out at the Oak Ridge National Laboratory (ORNL), on the attenuation of fission neutrons in water, it was found

that the insertion of relatively thin slabs of material between a fission source and a thick water shield gives an effect that can be correlated by a simple exponential attenuation factor that is characteristic of absorption processes alone. This behaviour might not be expected since nonabsorption effects predominate in fast neutron attenuation. However, the large thickness of water, *filters out* the neutrons deflected by the sample and thereby effects their complete removal. As a consequence, the effect of slabs of shield materials when followed by large thicknesses of hydrogeneous material can be described by an "equivalent absorption cross section averaged over energy", called *the removal cross section.*

The experimental set up is shown in Fig. 3.12. A beam of thermal neutrons from a reactor *thermal column* fall onto a disc of enriched uranium which is located at the one end of a large tank of water, the one, which is in contact with the thermal column. This tank is known as *the Lid Tank Shield Facility.* The thermal neutrons induce fissions in the uranium, and in this way the disc becomes an isotropic source of fission neutrons in water. The flux of fast neutrons, that is neutrons with energies greater than about 1 MeV, which have "survived" from interactions with the interposed materials, was measured at a distance r greater than about 60 cm.

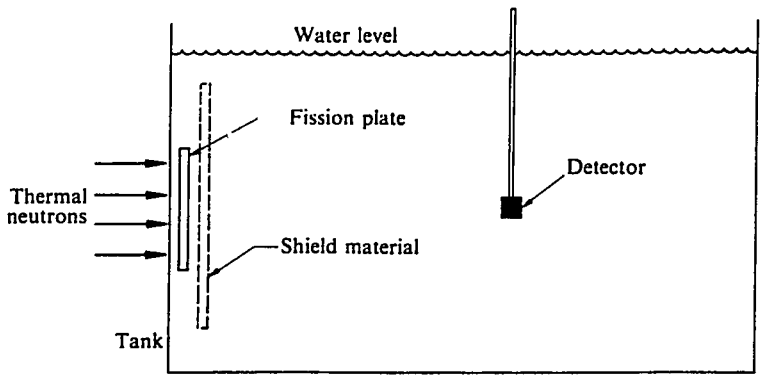

Fig. 3.12 The experimental facility at ORNL for the study of the attenuation of fission neutrons in water.

From experiments performed only with water between the neutron source and the detector at various distances from the source, it was found that the flux G(r) as a function of distance r from a "point" fission source, emitting isotropically one fission neutron per sec, can be represented by:

$$G(r) = \frac{A \cdot e^{-\Sigma_{R,w} \cdot r}}{4\pi r^2} \qquad (3.48)$$

where the constants A and $\Sigma_{R,w}$, as deduced from the experimental results,

have the values:

$$A = 0.12 \quad \text{and} \quad \Sigma_{R,w} = 0.103 \text{ cm}^{-1} \tag{3.49}$$

The function G(r) is known as *the point water kernel.*

This form of G(r) suggests that far from the source (i.e. for r: $r \geq 45$ cm) the source neutrons are absorbed with an *effective macroscopic absorption cross section* $\Sigma_{R,w}$. What in fact is happening is that the neutrons are being *removed* (from the group of neutrons with energies greater than 1 MeV) as the result of scattering in the water, and for this reason $\Sigma_{R,w}$ is called *the macroscopic removal cross section of fission neutrons for water.*

From experiments performed by placing successively slabs of a certain material, of various thicknesses in front of the fission plate, it was found that the neutron flux at the constant point where the detector is positioned, follows an exponential law, i.e.:

$$\Phi(r,d) = S_S \cdot G(r) \cdot e^{-\Sigma_R d} \tag{3.50}$$

where: S_S , is the source strength (fission neutrons/cm^2 sec),
$G(r)$, is the point water kernel,
Σ_R , is the macroscopic removal cross section of fission neutrons for the material in question, and
d , is the slab thickness.

Values of Σ_R were estimated from the experimental results performed with various slab materials. These results for σ_R ($\sigma_R = \Sigma_R/N$), *the microscopic removal cross section for fission neutrons* are given in Table 3.4.

Table 3.4 Microscopic removal cross sections of various elements and compounds, measured at the ORNL facility.

Material	σ_R, b/atom	Material	σ_R, b/atom
Aluminum	1.31 ± 0.05	Tungsten	3.36
Beryllium	1.07 ± 0.06	Zirconium	2.36 ± 0.12
Bismuth	3.49 ± 0.35	Uranium	3.6 ± 0.4
Boron	0.97 ± 0.10	Boric oxide, B_2O_3	4.30 ± 0.41
Carbon	0.81 ± 0.05	Boron carbide, B_4C	4.7 ± 0.3
Chlorine	1.2 ± 0.8	Fluorothene, C_2F_3Cl	6.66 ± 0.8
Copper	2.04 ± 0.11	Heavy water, D_2O	2.76 ± 0.11
Fluorine	1.29 ± 0.06	Hevimet (90 wt.% W,	
Iron	1.98 ± 0.08	6 wt.% Ni, 4 wt.% Cu)	3.22 ± 0.18
Lead	3.53 ± 0.30	Lithium fluoride, LiF	2.43 ± 0.34
Lithium	1.01 ± 0.05	Oil, CH_2	2.84 ± 0.11
Nickel	1.89 ± 0.10	Paraffin, $C_{30}H_{62}$	80.5 ± 5.2
Oxygen	0.99 ± 0.10	Perfluoroheptane, C_7F_{16}	26.3 ± 0.8

From equ. (3.50) one can deduce the following expression for the *modified point kernel function*, taking in account the presence of the shield slab:

$$G'(r,d) = \frac{A \cdot e^{-\Sigma_{R,w}(r-d)}}{4\pi r^2} \cdot e^{-\Sigma_R d} \qquad (3.51)$$

The above mentioned accreditations constitute the known as " removal theory".

3.5.3 Some applications of the removal theory.

In the following, some examples will be given, refering to the application of the removal theory to some practical problems.

(a) Calculation of the neutron flux from a disc source of fission neutrons in water.

We consider the disc of fissionable material of radius R, of source strength S_f (fissions/cm^2·sec), immersed in a tank of water of large dimensions. The flux $\Phi(r)$ at point P on the axis of the disc (see Fig. 3.13), is calculated by using the expression for the point water kernel (3.48),

$$\Phi(r) = \frac{S_S \cdot A}{4\pi} \int_0^{2\pi} \int_r^{\sqrt{R^2+r^2}} \frac{e^{-\Sigma_{R,w} \cdot \rho}}{\rho^2} \cdot dS \qquad (3.52)$$

where: $S_S = \nu \cdot S_f$ is the strength of the source in fission neutrons/cm^2·sec,
ν , is the average number of neutrons ejected per fission, and
$dS = \rho \cdot d\rho \cdot d\varphi$, is the differential source surface.

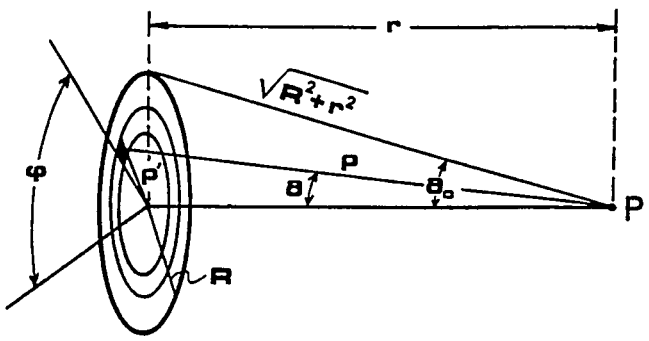

Fig. 3.13 For the calculation of the neutron flux from a disc source of fission neutrons in water.

Equation (3.52) gives:

$$\Phi(r) = \frac{\nu \cdot S_f A}{4\pi} \cdot \int_0^{2\pi} d\varphi \cdot \int_r^{r \cdot \sec\vartheta_0} \frac{e^{-\Sigma_{R,w} \cdot \rho}}{\rho} \cdot d\rho =$$

$$= \frac{\nu \cdot S_f A}{4\pi} \cdot [\, E_1(\Sigma_{R,w} \cdot r) - E_1(\Sigma_{R,w} \cdot r \cdot \sec\theta_0)] \qquad (3.53)$$

where: $$\sec\theta_0 = \sqrt{1 + (R/r)^2} \qquad (3.54)$$

and, $$E_1(x) = \int_x^{\infty} \frac{e^{-t}}{t} \cdot dt \qquad (3.55)$$

(b) Calculation of the neutron flux from a disc source of fission neutrons in water and beyond a slab of thickness d.

With the slab inserted between the disc source of the previous case and the detector at point P (as shown in Fig. 3.14) in water, the flux at P will be, according to the "point kernel technique",

$$\Phi(r,d) = \frac{\nu \cdot S_f \cdot A}{4\pi} \cdot \int_0^{2\pi} d\varphi \cdot \int_r^{r \cdot \sec\theta_0} \frac{e^{-\Sigma_{R,w} \cdot (\rho - d) \cdot \sec\vartheta} \cdot e^{-\Sigma_R \cdot d \cdot \sec\vartheta}}{\rho} \cdot d\rho$$

$$= \frac{\nu \cdot S_f \cdot A}{4\pi} \cdot E_1[\Sigma_{R,w}(r - d) + \Sigma_R\, d] - E_1[\Sigma_{R,w}(r - d)\sec\theta_0 + \Sigma_R\, d \sec\theta_0] \qquad (3.56)$$

where, Σ_R is the macroscopic removal cross section for fission neutrons of the heavy material of the slab.

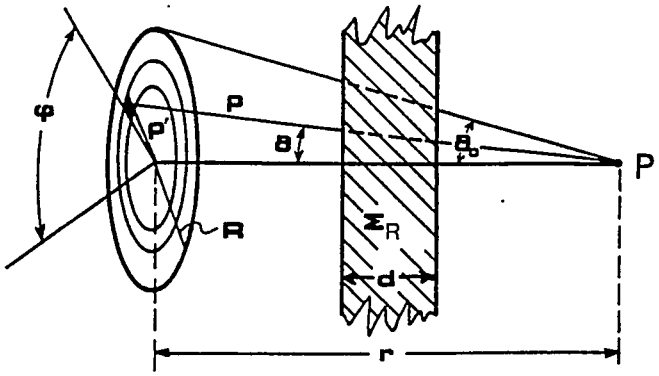

Fig. 3.14 For the calculation of the neutron flux, from a disc source of fission neutrons in water and beyond a slab of material.

(c) Approximate calculation of the neutron flux, out of the shield of a spherical homogeneous nuclear reactor.

We consider the spherical reactor, consisting of a core of radius R surrounded by a hydrogeneous shield (water) of thickness "a", as shown in Fig. 3.15. The core consists of a mixture of metal (fuel) and water (moderator) with the

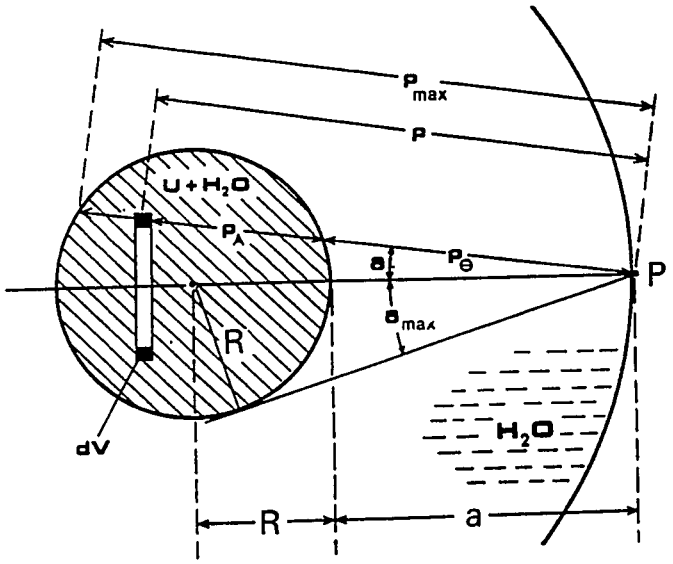

Fig. 3.15 Spherical reactor core shielded by a spherical geometry water shield.

volume fraction of metal equal to f_m. It will be assumed, for simplicity that the fission neutrons are being produced uniformly throughout the core at the rate of S_V neutrons/cm^3·sec.

The fast neutron flux at the point P on the surface of the shield can be computed by the usual "point kernel technique" i.e., by adding up the contributions to the flux from volume elements dV within the core. In view of the symmetry of the problem, the appropriate volume element is that of a ring whose volume is,

$$dV = 2\cdot\pi\cdot\rho^2\cdot\sin\theta\cdot d\theta\cdot d\rho \tag{3.57}$$

and its intensity is $S_V\cdot dV$.

The differential flux at point P from the elementary source $S_V\cdot dV$ is:

$$d\Phi_P = \frac{A\cdot S_V\cdot dV}{4\pi\rho^2}\cdot e^{-(1-f_m)\Sigma_{R,w}\rho_A}\cdot e^{-f_m\Sigma_{R,m}\rho_A}\cdot e^{-\Sigma_{R,w}\rho_\Theta} \tag{3.58}$$

where: $\Sigma_{R,m}$ is the macroscopic removal cross section for fission neutrons of the metallic fuel,

$\Sigma_{R,w}$ is the macroscopic removal cross section for fission neutrons of the water,

ρ_A, ρ_Θ (where: $\rho_A + \rho_\Theta = \rho$) are the shown in Fig. 3.15 distances,

$(1-f_m)\cdot\Sigma_{R,w}$ is the "partial" macroscopic removal cross section for the water in the homogeneous mixture of the core, and

$f_m\cdot\Sigma_{R,m}$ is the "partial" macroscopic removal cross section for the metallic fuel material in the homogeneous mixture of the core.

Substituting in equation (3.58):

$$\rho_A = \rho - \rho_\Theta \tag{3.59}$$

$$\alpha = (1-f_m)\cdot\Sigma_{R,w} + f_m\cdot\Sigma_{R,m} \tag{3.60}$$

and,

$$\beta = \Sigma_{R,w} - (1-f_m)\cdot\Sigma_{R,w} - f_m\cdot\Sigma_{R,m} \tag{3.61}$$

we obtain:

$$d\Phi_P = \frac{A\cdot S_V\cdot dV}{4\pi\rho^2}\cdot e^{-(\alpha\rho+\beta\rho_\Theta)} \tag{3.62}$$

Substituting in equ. (3.62) the expression (3.57) for dV and integrating over the whole volume of the core, we obtain:

$$\Phi_P = \frac{A\cdot S_V}{2}\cdot\int_0^{\vartheta_{max}}\sin\vartheta\cdot d\vartheta\cdot\int_{\rho_\Theta}^{\rho_{max}} e^{-(\alpha\rho+\beta\rho_\Theta)}\cdot d\rho \tag{3.63}$$

where:

$$\theta_{max} = \arcsin\left(\frac{R}{R+a}\right) \tag{3.64}$$

the maximum value of θ, and

$$\rho_{max} = (R+a)\cos\theta + \sqrt{R^2-(R+a)^2\cdot\sin^2\theta} \tag{3.65}$$

the maximum value of ρ for a given angle θ.

While ρ_Θ is a function of θ, it is independent of ρ and is therefore held constant during the ρ-integration in equ. (3.63). Carrying out this integration we obtain:

$$\Phi_P = \frac{A\cdot S_V}{2\alpha}\cdot\int_0^{\vartheta_{max}}(e^{-\alpha\cdot\rho_\Theta} - e^{-\alpha\rho_{max}})\cdot e^{-\beta\rho_\Theta}\cdot\sin\theta\cdot d\theta \tag{3.66}$$

The remaining integral cannot be performed analytically and must be calculated numerically. However, in the case of a small core and a thick shield, the integral can be approximated by taking:

$$\sin\theta \simeq \theta$$

$$\theta_{max} \simeq \frac{R}{R+a}$$

$$\rho_\Theta \simeq a$$

$$\rho_{max} \simeq 2R + a$$

Equation (3.66) then reduces to,

$$\Phi_P = \frac{A \cdot S_V}{2\alpha} \cdot e^{-(\alpha+\beta)a} \cdot (1 - e^{-2\alpha R}) \cdot \int_0^{\vartheta_{max}} \theta \cdot d\theta \qquad (3.68)$$

or, given that: $\alpha + \beta = \Sigma_{R,w}$,

$$\Phi_P = \frac{A \cdot S_V}{4\alpha} \cdot \left(\frac{R}{R+a}\right)^2 \cdot e^{-\Sigma_{R,w} a} \cdot (1 - e^{-2\alpha R}) \qquad (3.69)$$

In the case that we want to take in account a layer of metal, say iron, of thickness t between the core and the water shielding, where $t << a$, then Φ_P is reduced by the factor $e^{-\Sigma_{R,Fe} t}$, that is:

$$\Phi_{P,\text{ with Fe}} = e^{-\Sigma_{R,Fe} \cdot t} \cdot \Phi_{P,\text{ without Fe}} \qquad (3.70)$$

References

1. Livingston, S. & H. Bethe, Revs. Modern Phys. 9 , 263 , (1937).
2. Beiser A., Revs. Modern Phys., 24 , 273, (1952).
3. Price W. J., Nuclear Radiation Detection, McGraw-Hill Inc., (1958).
4. Sachs D.S., & J.R. Richardson, Phys. Rev., 83, 834 ,(1951).
5. Siegbahn K., α,β,γ Ray Spectroscopy, Vol.I., North Holland, (1974).
6. Evans R.D., The Atonic Nucleus, McGraw-Hill Inc., (1955).
7. Lamarsh J.R., Introduction to Nuclear Engineering, Addison-Wesley, (1983).
8. Katcoff S.J., J.A. Miskel & C.W. Stanley, Phys. Rev. 74, 631, (1948).
9. Alexander J.M., & M.F. Gazdik, Phys. Rev. 120, 874, (1960).
10. Segré E., Experimental Nuclear Physics, Vol.I., John Wiley & Sons, (1960).
11. Katz L. & A.S. Penfold., Revs. Mod. Phys. 24(I), 28, (1952).
12. Gol'din M.L., & V.D. Tkachenko, Soviet Atomic Energy 52 (2) ,144, (1982).
13. Frank I., & I. Tamm, Compt. rend. acad. sci URSS , 14, 109, (1937).
14. Fano U., Nucleonics, 11, 8 , (1953).
15. Etherington H., Nuclear Eng. Hanbook , Mc-Graw Hill Co., (1958).
16. Klein O., & Y. Nishina, Z. Physik , 52, 853, (1929).
17. Rockwell Th., Editor, Reactor Shielding Design Manual, Mc-Millan .
18. Jaeger R.G., Engineering Compendium on Radiation Shielding VIII, Springer--Verlag, (1968).